OFFICE OF NAVAL RESEARCH

Number 3511 (00) Project Number 051 - 380

THEORETICAL AND EXPERIMENTAL INVESTIGATIONS OF THE LIGHT SCATTERING OF COLLOIDAL SPHERES

BY

WILFRIED HELLER

TECHNICAL REPORT NO. 3 (49)

November 15, 1962

Submitted by

W. Heller, Project Director

Department of Chemistry

Wayne State University

Detroit 2, Michigan

The enclosed little article has been written on request for "Naval Research Reviews". The actual publication, in the present or in a revised form, is, of course, subject to the decision to be made by the editor.

W. H.

RADIATION SCATTERING, YESTERDAY'S CINDERELLA, TODAY'S PRIMADONNA

Wilfried Heller
Department of Chemistry
Wayne State University
Detroit 2, Michigan

In 1870 and 1871 the Franco-Prussian war was raging on the continent of Europe and many Englishmen were deeply concerned about the effect of the outcome on the continental balance of power. One Englishman, J. W. Strutt, however, was concerned about an entirely different matter. He was wondering why the sky is blue during the day since in absence of any reflecting matter in the atmosphere one would have expected it to be pitch black. While Wilhelm I and Napoleon III tried to make political history, Mr. Strutt made real history by developing a theory intended to solve the mystery of the sky's coloration. Now, 90 years later, one realizes how tremendous a breakthrough Strutt's theory represented. It is to the credit of Queen Victoria that, here again, she proved to be very far-sighted because Mr. Strutt was soon to be knighted i. e. he was allowed, in 1873, to assume the title of his father, Lord Rayleigh.

Rayleigh had postulated a new phenomenon in order to account for the blue of the sky: light scattering. He assumed that the individual molecules in the atmosphere on being illuminated by the sun scatter in all directions a minute fraction of the radiation received. Assuming that each molecule behaves, under the influence of incident radiation, like a single induced dipole, he calculated the nature of the effect to be expected and found it to be essentially in agreement with the facts. According to his theory, which he later refined, the intensity of the light scattered from an incident light beam should increase with the inverse fourth power of the wavelength of the latter, with the sixth power of the radius of the scattering material - assuming it to be spherical in shape - and should increase also with the refractive index ratio of the scatterer and its surroundings.

Since the sun emits a continuous spectrum (except for the Fraunhofer lines), the inverse fourth power law shows at once that scattered blue sunlight (4500 A) will be more than three times as intense as scattered red sunlight (6000 A) on assuming, for simplicity sake, spectral invariance of the sun's brightness within these limits. The blue color of the sky was thus explained quantitatively. In addition, if anyone would have asked Lord Rayleigh in 1871 as to what the earth would look like from outer space he probably would have answered without hesitation that the earth must look like a ball surrounded by a very beautiful bluish violet halo, whenever direct sunlight does not interfere with the observation. This in fact has been observed by Glenn on his orbital flight and by the others who preceded and followed him. (The June, 1962 issue of the National Geographic Magazine gives on pages 808-810 beautiful color photographs of this halo as taken by Colonel Glenn.) An obvious corollary of this preferential blue scattering is the fact, well known to all of us, that the sun itself may look reddish during the sunset or sunrise, i.e. if it is viewed through thick enough layers of scattering material (through the maximal optical thickness of the atmosphere plus haze). This better penetration of long wavelength radiation through haze is the simple reason for using infrared photography for objects obscured by haze or clouds. The strong increase of Rayleigh scattering with particle size explains readily why the relatively small amount of tiny smoke particles rising from the burning end of a cigar or cigarette viewed laterally in ordinary daylight gives rise to a relatively intense beam of scattered blue light, while, on the other hand, a tremendously large number of molecules of nitrogen and oxygen in the atmosphere, i.e. an appreciable atmospheric thickness, are required to lead to the same effect on viewing the sky. The importance of the refractive index difference between scatterer and environment may also be demonstrated by a simple experiment which everyone of us has carried out, involuntarily, at one time or another. A sheet of typewriter paper soiled with a speck of butter from

a sandwich becomes transparent where it has been touched. Typewriter paper is opaque due only to light scattering by a dense network of fully transparent fibers. By substituting fat for air as the medium in which the fibers are embedded, the ratio of the refractive indices is reduced from 1.55 ± 0.03 to 1.06 and this, in turn, reduces the scattering appreciably (the refractive indices involved are: cellulose, 1.55 ± 0.03; butterfat, 1.46; air, around 1.00). To be sure, the scattering process is far more complex here, the particles being very large, non-spherical, and intertwinded which causes interference phenomena. However, the refractive index effect is here, qualitatively, the same as in the simpler case of Rayleigh scattering. (In the case of Rayleigh scattering, the reduction in the refractive index ratio indicated would lead to a more than thousand fold increase in transmittancy.)

Those who have performed, before reading this far, the scattering experiment with cigar or cigarette smoke may have noticed that the smoke coming out from the end opposite to the burning end has a grayish or brownish color. While one has, here again, an effect of light scattering, it does clearly not fall within the range of the Rayleigh theory. The smoke particles in this instance are far too large to be considered as single dipoles. As a rule of thumb one can say that the Rayleigh theory will fail if the longest dimension of the scatterers exceeds about 1/20 of the wavelength of the radiation used. While the blue smoke therefore consists of particles smaller than 1 millionth of an inch, the particles in the gray smoke are appreciably larger and are probably of the order of hundreth thousandths of an inch. (This is the result of particle aggregration during the transport of smoke through the tobacco.) Another common example of scattering by relatively large particles is the grayish ray of light coming through a tall church window. Here, the scattering particles are dust particles. While gray coloration of the scattered light is the phenomenon generally observed if the relatively large

particles are present in various sizes, singularly striking colors of any hue in the spectrum are likely if they all have approximately the same size. This, for instance, is the cause and the prerequisite of the beautiful multicolored sunsets occasionally observed, particularly if the lower layers of the atmosphere and peripheral areas around clouds contain a large amount of tiny water droplets of about the same size. These larger particles in the lower atmosphere are, of course, also responsible for the red, yellow and gray bands which are seen from outer space between the blue Rayleigh halo and the boundary of the earth (see the photographs referred to above). It is fairly easy to anticipate that these non-blue bands will be more prominent over heavily populated areas than over desolate areas and oceans. In addition to the complicated spectral variation of scattered light, one observes with relatively large particles several other characteristically different scattering properties. Among them three are particularly noteworthy. First, the light scattered in the forward direction, i.e. in the same direction traveled by the incident radiation is larger than that scattered in the backward direction. This lopsidedness increases rapidly with size. (In contradistinction, Rayleigh scattering in the forward and backward direction are equal.) The next time you are driving in misty weather up towards the crest of a hill you will want to verify this preferential forward scattering by the following simple observation: a car which is travelling towards you, but is still out of sight below the crest of the hill, sends up an impressively bright beam of light; a car travelling ahead of you in the same direction in which you are going will also send a beam of light up into the sky but this scattered beam, viewed by you of course in the backward direction, is incomparably weaker. The second noteworthy difference in the scattering by relatively large particles is that the total amount of light scattered by a system of given

concentration of scatterers per unit volume reaches a maximum value at a very specific intermediate particle size. For this phenomenon also one can cite a common experience: the brightness of a distant light source or the visibility of a distant illuminated object are minimal in fog while they are better both in misty weather and in a heavy drizzle. The average water droplet size in fog is intermediate between that in the two other instances and it is such that it produces the maximal hiding power. The implications for the production of smoke screens of maximum efficiency are obvious. The third interesting difference in the scattering by relatively large particles is the fact that the scattered light observed at an angle of 90° with respect to the incident beam will be found to be only partially polarized while Rayleigh scattering is, for the same angle of observation, fully polarized. This phenomenon is outside of the realm of easy everyday experience, but its practical significance and importance ranks with the others enumerated.

The problem of the theory of scattering by particles which are not small compared to the wavelength can be divided into two cases. The first is that of spheres. All possible contingencies that may arise here are taken care of by a theory developed by Mie in 1908. However, the extraordinary difficulties arising in actual calculations have delayed its full scale application until electronic computers became available. The second case is that of nonspherical particles. Here also a most useful theory exists, again initiated by Rayleigh (1911). It is, however, applicable only in the limiting case that the refractive index of the scattering material differs very little from that of the surroundings. Very slowly progress is being made in developing theories in which this limitation will be reduced gradually. In the meantime, one must be satisfied with various approximating treatments.

The great importance of light scattering derives from the fact that it

allows one to investigate quantitatively an amazingly large number of problems in many fields of human endeavor. This can be done without interfering in any way with the system investigated. One of the reasons for this unique position of the light scattering method as an analytical tool is the fact that there is, in principle, no limitation as to the wavelength that may be used. The phenomena tractable by the existing theories are the same no matter whether the radiation is that of visible light, or is of shorter wavelength (ultraviolet, X-rays, gamma radiation), or longer wavelength (infrared, far infrared, radar or broadcasting waves). This is due to the fact that the absolute size of particles does not matter, only the size relative to the wavelength is important. Thus, hollow Al- spheres one inch in diameter strewn into the atmosphere will scatter, i.e. attenuate radar waves quantitatively exactly like tiny Al- spheres, one tenthousandths of an inch in diameter, will scatter visible light provided only that differences in the refractive indices at the two wavelengths are taken into account.

On reviewing the development of science, technology and national defense, during the last fifteen years, it is amazing to see how large a contribution the understanding and the application of radiation scattering has made in all these areas. The space available here allows one to give only a few significant examples. The amazing progress in the fields of polymer chemistry and biochemistry is to a large extent due to the fact that light scattering has provided a rapid, reliable and precise method for determining molecular weights and approximate molecular shapes and has allowed one, what no other method is capable of doing, to follow the kinetics of changes in these qualities. Noteworthy here is the pioneering work by Zimm and by Doty in the late forties. In all these areas, it is primarily Rayleigh scattering which has, at last, taken its place as a tool in scientific research which it so fully deserves. A large part of the credit for this goes to Debye who, in 1943, put the final touches to a theory

developed by Einstein in 1910. This theory, though based upon an entirely different approach, is fully equivalent to Rayleigh's theory. It has, however, the advantage that the final equations arrived at facilitate the practical application of the scattering effect and furthermore allow one to obtain, in addition to the primary information on molecular weights and shapes, information on the thermodynamics of the systems and processes studied. In the field of colloid chemistry which deals with particles too small to be seen in a microscope, but larger than an average macromolecule, the growing exploitation of the Mie theory has put us just now on the threshold of a full understanding and control of the behavior of emulsions and of aerosols, to name only two important classes of systems in this area. (Experimentally, the work on scattering by aerosols was initiated in this country primarily by La Mer [1943].) In various laboratories, extensive theoretical work is underway concerned with the quantitative evaluation of radar attenuation by tiny atmospheric ice crystals and by various types of cloud formations One also has available now complete theoretical information (results of the writer published thus far only in preliminary form) which will allow one to predict the exact range of particle sizes which for a given wavelength in the visible range, in the range of radar waves or of broadcasting waves, will lead to minimum radiation transmission or maximum radiation reflection. These and other developments in the science of light scattering hold the promise of a more fruitful investigation of fogs and smogs. A full understanding that thus may be achieved, certainly will be the decisive step towards eventual control or complete eradication. Fog and smog are the ultimate result of a large accummulation in the lower atmosphere of dust and debris from combustion which act as nuclei for water condensation. However, the conclusion that the upper atmosphere is pure and clean would not be

justified. Light scattering experiments quite recently showed that dust may be carried by eddy currents as high as 80,000 feet. This finding, incidentally, leads to a solution of the puzzling problem as to why the sky is brighter than one would expect from Rayleigh's theory. Investigations by space probes gave exactly the same results on the pollution of the upper atmosphere, the only difference being that light scattering gave this information at a considerably smaller cost.

The sky, however, is not the limit for scattering enthusiasts. They already are busily engaged in wresting from outer space many of its secrets without having to take their feet off the ground. One hopes to clear up by scattering experiments the unknown depth and concentration of the atmosphere of Venus by studying its effect upon a beam reflected from the surface of the planet. It also is reasonable to expect that scattering may give useful information on the consistency of the surface of the moon which is being debated so much. No attempts in this direction seem to have been made thus far. Light scattering work has also begun to extend beyond the reaches of our solar system. Particularly fascinating is the work of the Belgian astrophysicist, Dr. Swings, on the radiation which comes to us from comets. Superimposed upon their discrete emission spectrum is a continuum which now has been found to be due to the scattering of sunlight by cometary dust. Moreover, this dust effect appears to be larger the older the comet. Therefore, a method is developing here which will allow one before too long to tell the age of a comet from the amount of dust it has managed to collect in its tail. Where all this dust comes from has also been partially explained by light scattering measurements. Thus, it has been found in England that the solar F-corona may be understood as the result of scattering by dust. The sun thus may turn out to be one of the dust generators,

while the comets may belong to the class of dust catchers. The "cosmic dust", as it is called, often is present in space in such large concentrations that it partially obscures the radiation from distant galaxies. These giant blobs also are the object of light scattering measurements in the hope to obtain further information on their mysteries.

Returning now to earth and proceeding in the opposite direction, i.e., entering the microcosmic world of the atomic nucleus, it is common knowledge that much of the progress made here is due to experiments with the cloud chamber and, more recently, with the bubble chamber. Here light scattering makes visible convincingly, though indirectly, the paths taken by α-particles, protons, electrons, positrons, mesons, and to follow the interactions of the so-called "strange particles" of nuclear physics. Phenomena such as neutron scattering also are treated by means of theories which in many respects are related to the scattering of electromagnetic waves. An application of scattering which is of particular concern to many of us is its use as a potentially powerful tool in medical diagnosis. One successful example dating back to the waning period of World War II is the examination of donor blood for the degree of non-sphericity of red blood cells by a rapid experiment on the deviation of lateral scattering from symmetry. Another example is the present, intriguing work by Boyle and associates who believe that the presence and development of atherosclerosis may be detected and studied by light scattering measurements on blood serum.

Rapidly developing also is the theory and practical application of light scattering of transparent or translucent solids. Here light scattering may be due to a dispersion, within the solid, of gases or of liquids or, it may be due to the formation of tiny regions of molecular orientation within the matrix

or it may, simply, result from internal strain or from cavities. In all these cases, internal refractive index differences arise and the resulting optical inhomogeneity leads to light scattering and, consequently, to more or less pronounced opaqueness. A good example of a solid rendered opaque by the entrapment of tiny droplets of water is the pearl. Its delicate bluish gray color originates exclusively from light scattering. (Therefore, you should never heat a pearl above the boiling point of water.) An example of light scattering due to differences in molecular orientation within a solid is the scattering by polymer films, studied in this country at present primarily by Stein and collaborators. It gives valuable information on the internal structure of polymer films. A lesson learned from the fact that inhomogeneities in solids may make them opaque, due only to refractive index differences, is that one now can make glasses, particularly plastic glasses, more transparent than before by simply eliminating or matching refractive index differences. One has even succeeded to manufacture translucent rubber tires by using exotic fillers instead of carbon black. Unfortunately, their mechanical properties still leave much to be desired. Once this bottleneck is ironed out, translucent tires may well become the next fad of car owners, particularly since white side walls have already become so common place that they can no longer be used as a mark of personal distinction. Into this category of light scattering phenomena belongs also the finite, although extremely weak scattering by liquids where it is due to local statistical density differences caused by the thermal motion of the molecules which make up the liquid. Of potentially far reaching theoretical importance here is the very recent attempt by Debye (1961) to use this phenomenon in order to obtain in liquid mixtures information on the range of molecular forces.

The radiation scattered by molecules, particles, or inhomogeneities has

thus far been considered as being unaffected by that scattered by neighbors. Actually there is an interference between the individual scattered wavelets, more so the smaller the distances of neighbors, relative to the dimension of the wavelength. A whole host of theoretically interesting and practically most important phenomena can result from such interferences. Some of them belong in an area which the uninquiring mind may wish to classify as a part of the "twilight zone". We will limit ourselves to a brief outline of the latter which are particularly intriguing.

When you drive along a highway on a hot summer day, you may see dark patches on it in the distance which look just like water. Then, when you come closer, they vanish. The next time when you make this observation, stop while you see these patches and wait until a car passes you and drives over those patches. You will be amazed to see that the car seems to lift itself a few inches off the ground and to travel in air. Moreover, you may see its understructure reflected on the patches. What is the reason? Within 2-3 inches off the ground, the temperature is 30° - 50° higher than further up. Due to the resulting refractive index differences, the thin hot air layer scatters quite differently than the air above it. This results in refraction and reflection. Although this is contrary to everyday experience, this phenomenon shows that not only solid surfaces, but surfaces separating gases of different optical properties, can produce perfect reflection due to the reason stated. The practical result, in the present instance, is the macroscopic effect of (a) invisibility of the ground proper and (b) reflection from the upper border of the hot air layer, provided only that the angle which the particular area on the highway makes with respect to both the sun and the direction of your vision is just right. Similarly you may, for the same reason,

on driving across Utah's Salt Lake on a hot afternoon, suddenly see one of the mountains on the horizon detach itself from its base, an experience which this writer will never forget. Flying saucers also belong into this category of phenomena, although here the diffuse reflection and refraction originate at the surfaces of vortices of the air which differ in density from the rest of the air. They are generally circular and, according to Helmholtz, may be extremely longlived. They may, therefore, have travelled far from the place where they were generated, for instance by a jet breaking the sound barrier. Unquestionably, photographs of this phenomenon could be taken if and when the density differences are large enough. Another phenomenon which is even more closely related to our "flying automobile" and which turned out to be of extreme practical usefulness, is that of transhorizon wave propagation, due to diffuse reflection on stratifications in the uppermost sections of the atmosphere. The closely related but optically more perfect phenomenon of fata morgana requires special temperature gradients similar to those which lead to the car riding in the air. We all have felt sympathy with the man lost in the Sahara desert who became elated on suddenly seeing the mirage of an oasis in the distant sky. Helas, we cannot control these phenomena yet, but eventually we may. If that happens, there is no way of predicting how real estate values in the Mojave desert will skyrocket since real estate agents may then be able to include in their package deal a permanent fata morgana in the backyard allowing a choice view of a selected section of Yosemite National Park.

INTRODUCTION

The present technical report is a survey article on the scattering by spheres to be published shortly in a book entitled "Electromagnetic Scattering" by Pergamon Press. It differs from the article in as much as section II has been eliminated and a few minor other cuts have been made in order to conform to the limits imposed upon the length of the individual contributions made to this book. The great majority of the theoretical and experimental results discussed in more detail are those arrived at by the Research staff of this laboratory under the Sponsorship of the Office of Naval Research.

The original Figure 5 was eliminated in this report because it would have required about 100 photographic reproductions. The Figure was not considered sufficiently important for an understanding of the text to burden the project with this extra expense. The elimination of this Figure led, however, to a mixup in some figure numbers, discovered after hectographing had been completed. In order not to delay issuance of this report any longer, an error guide is inserted on the following page which should exclude any possibility of confusion.

It should be noted that Figures 3, and 4, which were oversized, have been split in halfs in order to insert them conveniently in this report. Figure 3 is split into an upper and a lower half. Figure 4 is split into a left hand side and right hand side half.

Corrections for Figure Numbers

Page	Read Instead of	Rather
19	Fig. 5	no Figure
21	Fig. 6	Fig. 5
22	Fig. 5	no Figure
24	Fig. 5c	no Figure
24	Fig. 7	Fig. 6
25	Fig. 8	Fig. 7
25	Fig. 9	Fig. 8

THEORETICAL AND EXPERIMENTAL INVESTIGATIONS OF THE LIGHT SCATTERING OF COLLOIDAL SPHERES

Wilfried Heller
Chemistry Department
Wayne State University
Detroit, Michigan

I Introduction

The most important theories on the scattering of electromagnetic radiation by spheres were developed prior to 1940, the first theory by Rayleigh[1] having been formulated more than 90 years ago. Experimentation in this field was also quite active between 1900 and 1940[2]. Large scale exploitation and refinements of existing theories and intensive experimental application of the scattering phenomena did not, however, get under-way until a year or two after the beginning of World War II. Only then were the potentialities of the light scattering method more fully recognized and taken advantage of in connection with pressing defense problems[3]. It is not possible within the space available here to do proper justice to all the excellent theoretical and experimental work that has been collected during the past twenty years on the scattering of spheres. The intention is rather to point out the most interesting new facts elicited from the theory, particularly from that of Mie[4], and the most promising experimental methods used in the recent past in order to take best advantage of the theory in the study of systems containing spheres.

II Essentials of the Theory of Scattering by Spheres

The scattering of a dielectric nonabsorbing sphere (conducting spheres will not be considered here) depends on two variables: 1) its size relative to the wave length of the electromagnetic radiation. It will be expressed in terms of $\alpha = 2 r_s \pi/\lambda$ where r_s is the radius of the sphere and λ is the wave length in the medium; 2) its dielectric constant, ε_2, relative to that of the surrounding medium, ε_1, which shall be expressed in terms of the relative refractive index, $m = n_2/n_1$, where n_2 and n_1 are the refractive indices

*This work was carried out with the support of the Office of Naval Research.

of the sphere and of the medium respectively, ($n^2 = \varepsilon$). In the simple case that $\alpha \to 0$, the radiation scattering by a sphere is that expected from oscillating dipole induced by the external electromagnetic field. This case is covered by the Rayleigh theory[1]. As long as the sphere is so small compared to the wave length that the phase of the exciting field is, at a given instant, virtually the same throughout the particle, isotropic inhomogeneities within the sphere do not affect the validity of the theory. However, they co-determine the effective value of n_2 and the absolute magnitude of scattering. Consequently, Debye's theory of light scattering by solutions[5], which was of decisive importance for the modern development of polymer chemistry, is fully equivalent to Rayleigh's theory. A randomly coiled dissolved macromolecule very small compared to the wave length will scatter radiation like a random assembly of spherical micro-beads (molecular segments) connected to each other by valence bonds. Here, as in the case of the actual Rayleigh sphere, one "collective" dipole represents quantitatively the contribution to scattering of all the volume elements (beads and solvent molecules contained with the quasispherical volume of the macromolecule)*.

Since the Rayleigh and Debye theories are valid only as long as $\alpha \to 0$, it is important to know how large α actually may be before a serious error is committed on using the equations arrived at in these theories. The total error in α-determinations by scattering measurements should not exceed 2% at the most, including the errors in measurements of the refractive index and of concentration. A deviation of 2% of α calculated from the Rayleigh equation is therefore a useful upper limit for the range of practical application of the Rayleigh or Debye theory.

---

*The interpretation of Debye scattering by macromolecules given here is, of course, different from but equivalent to that actually underlying the Debye-Einstein theory, namely that the scattering effect may be considered as the result of fluctuations in concentration (see e.g. (6)).

On this basis, the upper limits are arrived at in Table I*. The limits of validity are given for the specific turbidity, defined in Section III. They are virtually the same for any other light scattering quantity**.

As the sphere becomes larger, it is no longer possible to replace the oscillators within it by a single representative dipole since there is now a finite phase shift, in the direction of the incident beam, in the oscillation of both the primary and the scattered electromagnetic field across the sphere. Consequently, in addition to the scattered wave of the single representative dipole, a second partial wave to be ascribed to the first electric quadrupole and a third, due to the first mangetic dipole, become now important. If the aim is merely a modest extension of the α -range accessible to quantitative treatment without imposing any restriction on the value of m, one may then make use of Stevenson's extension of the Rayleigh theory[7], in which precisely these second and third partial waves are taken into account. The Stevenson equation extends the range of particle sizes accessible to quantitative determinations two to three fold depending on the value of m[6].

For still larger particles additional partial waves make finite contributions to the scattered wave. Now, one can obtain relatively simple relations only provided it is assumed that $(m-1) \to 0$. This, of course, implies the assumption that the electromagnetic field inside the particle is the same as outside and is homogeneous throughout. The best known theories developed for this limiting case are those of Rayleigh[8] and of Gans[9], commonly referred to jointly as the Rayleigh-Gans theory and the second (chronologically first) theory of Debye[10].

---

*The α -values arrived at by means of the Mie-equation (see Section III) are considered here as the true α -values.

**The percent deviation depends on the scattering quantity considered, to a significant extent, only if its admissible value is set, at least, at 5%.

In the Rayleigh-Gans theory, the scattering functions arrived at may be considered as the resultant of the contributions of dipolar, quadrupolar, octopolar and higher polar partial waves, both electric and magnetic. In the Debye theory (which originated with the scattering of X-rays), the elementary concept of exclusive dipolar radiation is maintained. However, a particle is now replaced by an array of dipoles whose coherent radiation is no longer in phase. The intensity of the radiation scattered in a given direction is therefore, in a first approximation, given by the collective interference of the wavelets emanating from the individual dipoles, each being representative of a volume element of the particle (or molecule) small compared to the wave length. The equations arrived at are fully equivalent to those derived from the Rayleigh-Gans equation. There is, however, one physically interesting difference: the factor P (see below) which is merely a mathematical quantity in the Rayliegh-Gans equation, assumes here the significance of an "interference factor"*.

A survey of the performance of the theories just outlined is given in Fig. 1, employing the principle of "error contour charts"[13]. The graphical results are based upon a comparison of the ($\lambda i'/c$) data obtained from the Mie-theory discussed below with those obtained from the other theories. Within each of the differently shaded areas the error is α, on using the respective theory

---

*Since the scattered wavelets are all in phase in the direction of the primary beam, P=1 in the forward direction. Consequently the light scattered in the forward direction is equal to that calculated from the Rayleigh theory for small spheres[1] provided, of course, that $(m-1) \rightarrow 0$. This forms the basis for Zimm's elegant method of determining large molecular weights by extrapolation of angular scattering intensities to the forward direction[11]. The Zimm method will, of course, be quantitatively correct only as long as a second type of interference effect, that between the scattered and primary beam in the forward direction, can be neglected, i.e. as long as (m-1) is very small and, in addition, as long as α is not very large[12].

is less than 5%. The contour line separating each shaded area from the rest of the diagram is the 5% deviation line; beyond it the deviation is $>$ 5%. (On considering a 2% deviation as the permissible maximum, each of the areas would be distinctly smaller.) The error contour charts are, obviously, somewhat different on considering, instead of $(\lambda\tau/c)$, angular scattering data, but the characteristic features of the contours are the same[14]. The following hitherto unknown and rather surprising facts emerge from the charts: 1) the range of α -values accessible by means of the Rayleigh theory increases significantly with m. (Beyond m = 1.35, however, the reverse trend manifests itself.); 2) the Rayleigh-Gans and Debye theories (to be referred to as R-G-D theory on account of their equivalence) are, within a narrow α -range (from about 2.0 to about 5.0), valid at m-values in excess of 1.10, and from an α of about 0.8 up to about 9.5 valid at m-values as large as 1.05. This defines, in practical terms, the consequence of the theoretical stipulation that $(m-1) \to 0$; 3) the R-G-D theory is limited to extremely small (m-1)-values at very low α -values which illustrates the grave risks involved in its application to polymer solutions.

For all those α - and m-values which are not covered by these three theories, one has to use the Mie-theory[4] if strictly accurate data are desired. The only exceptions are very large α-values (larger than about 50) where formalistic treatments based upon or related to geometrical optics may be quantitatively adequate. The Mie theory takes implicitly full account of the following complications which arise when neither $\alpha \to 0$ nor $(m-1) \to 0$: 1) the amplitude of the oscillations (the electric and magnetic field strengths) within the sphere differs from that in the medium and a phase shift occurs at the boundary between medium and sphere; 2) the wave length within the sphere differs from that in the medium; 3) the phase of the exciting field and, consequently the phase of the scattered field, is, at any instant, different in different volume elements of the sphere, more so the larger the sphere; 4) the scattered field affects the primary

electromagnetic field. The restriction imposed in the Rayleigh theory that $\alpha \to 0$ allows one to disregard complications (3) and (4); the restriction imposed in the R-G-D theory that $(m-1) \to 0$ allows one to disregard complications (1), (2), and (4). Factor (2) and the resulting inhomogeneity of the electric field inside the particle* lead to depolarization, an effect which therefore is not accounted for in the R-G-D theory**. Factor (3) leads to ellipitically polarized light except for observation at 90° with respect to the incident beam, and also except for (indirect) observation in the forward and backward direction if the electric vector of the incident beam forms an angle differing from both 0° and 90° with the plane of observation. Factor (4) is responsible for complications in the determination of the refractive index of strongly scattering dissolved or dispersed material[14a].

The mathematical expressions at which Mie arrives are unfortunately very complicated. Therefore, except for some reasonably systematic, exploratory computations of light scattering functions by Blumer[15], relatively little computational work was done prior to 1945. The advent of electronic computers decisively changed this situation. The first systematic electronic computation, still of relatively modest scope by Lowan[16], was followed by the first large

---

*One may with certain reservations on account of the smallness of the scatterers unless $\alpha \gg 100$. Talk instead of the distortion of the wave front first in the scattering sphere. The front is no longer on a straight line perpendicular to the incident beam, but is curved.

**This is probably the most serious shortcoming of the R-G-D theory. Since the R-G-D theory has, on the other hand, the great advantage of not being restricted to spherical particles as the Mie theory is, attempts have been made in this laboratory to remove, at least partially, the shortcoming cited. One of two attempts aimed in this direction, that by Y. Ikeda is described elsewhere in this volume. The other by A. F. Stevenson, will be described in due time elsewhere.

scale evaluation for m-values ≥ 1.33[17] (which are of interest primarily for aerosols), and for m-values ≤ 1.30 (which are primarily of interest for liquid suspensions of spheres)[18]. Since interpolations of scattering functions are rather difficult at large m-values where all the functions oscillate extensively with both α and m, additional very elaborate computations for m-values ≥ 1.30[19] represent a most important addition to the tabular material provided by Sliepcevich. Taking into account also recent tabulations for special α - and m-values[20], one can say that the practical use of the Mie theory is now assured for virtually any α - and m-value which one may ordinarily expect to encounter for dielectric spheres on using light waves. An important initial step in computing Mie-functions for selectively absorbing spheres has also been made recently[21]. Similarly, as yet unpublished computations are being carried out by various authors in a large scale attempt to cover those special m-values which are of particular interest in microwave scattering and in space physics and meterology[22] to the extent that Penndorf's computations do not cover them as yet as fully as desirable.

In view of the extensive tabulations of scattering functions on the basis of the Mie theory, a series of approximating theoretical treatments, intended to be partial substitutes for the Mie theory, have lost their previous interest as far as the scattering of spheres is concerned. Some of them retain, however, considerable interest on account of their potential or actual applicability to the scattering by nonspherical bodies*. Particularly noteworthy for this reason are the following theories: 1) a theory by Hart and Montroll[23] which is comparable to the R-G-D theory in as much as the field strength (amplitude) in the particle and medium is assumed to be the same, but differs from it by assuming that the

---

*For such bodies, the development of an equivalent to the Mie theory, although attempted[22a], can hardly be hoped for in view of the quite extraordinary mathematical difficulties which are encountered.

wave length in the particle and medium differs. An error contour chart would probably show a slightly better performance than that found for the R-G-D theory; 2) a theory by van de Hulst[24] in which the phase shift in the primary electromagnetic field at the surface of the scattering particle is taken into account, while, on the other hand, both field strength and wave length are assumed to be the same in particle and medium. This theory also is apt to show a slightly better performance than the R-G-D theory.

Two other types of approximating treatments specifically concentrate on simplifying the Mie-expressions. One, by van de Hulst[24], is based on neglecting in a series development of the Mie equations those terms which at large α-values contribute relatively little so that "smoothed out" scattering curves are obtained. This approach allows one to define in good approximation the α- and m-values at which maxima and minima of the scattering coefficient and of the angular scattering occur (see Section IV for a definition of these terms). Related in purpose is a second simplifying treatment by Hart and Montroll pertinent to large α-values[23].

The same objectives aimed at by the two preceeding treatments can be achieved by substituting, whenever possible, for the Mie-functions analytical expressions derived from data actually computed from the Mie-theory. They necessarily neglect the small "wiggles" in the Mie-curves but obviously, give accurate results within the α- and m-range or ranges of their validity. Thus, Fig. 1 shows the α-m-area within which several suitable chosen analytical expressions duplicate the results of the Mie-turbidity data[25]. Similarly, the variation of the turbidity maximum (or of the prominent first maximum in the scattering coefficient) with α and m can easily be expressed by simple analytical expressions[26]. Lastly, the location of angular maxima and minima

follow relatively simple analytical expressions[27,28] as long as m is not too large.

III Formulation of the Practically Important Expressions with Emphasis on those Derived from the Mie Theory

Since several excellent threatises describe the essentials of the mathematical treatment by Mie[29], it is sufficient here to develop those final equations which are of direct experimental interest. For the sake of uniformity, the symbolism introduced by Mie will be adhered to as far as is practical.

The basic dimensionless quantity obtained from the Mie theory is i. It is a function of α, m and αm and its calculation involves the use of Bessel functions and Legendre polynomials. Depending on whether the electric vector of the incident linearly polarized beam vibrates perpendicular ($i_\perp$) or parallel ($i_\parallel$) relative to the plane of observation, the Mie theory yields

$$i_\perp(\gamma) = \left| \sum_{n=1}^{\infty} \left[\left\{ A_n P_n'(\cos\gamma)/\sin\gamma \right\} + B_n \, d P_n'(\cos\gamma)/d\gamma \right] \right|^2 \qquad (1)$$

$$i_\parallel(\gamma) = \left| \sum_{n=1}^{\infty} \left| \left\{ A_n \, d P_n'(\cos\gamma)/d\gamma \right\} + B_n \, P_n'(\cos\gamma)/\sin\gamma \right| \right|^2 \qquad (2)$$

Here γ is the angle of observation with respect to the reverse direction of the primary beam*. Since the full definition of the quantities A_n, B_n and P_n^1 is quite space consuming, the reader is referred to one of the repeated definitions given in the literature[31]. All practically important equations are directly derivable from eqs. (1) and (2). Considering first the radiant energy scattered by a single sphere in the direction γ, assuming the incident

---

*It is more common at present to use instead of the Mie-angle γ rather the angle between the direction of observation and the direction of the primary beam, Θ. Obviously, $\Theta = \pi - \gamma$.

beam to have unit intensity, one has the relations

$$J_{\perp}(\gamma) = \frac{\lambda^2}{4\pi^2 r^2} i_{\perp}(\gamma), \tag{3}$$

$$J_{\parallel}(\gamma) = \frac{\lambda^2}{4\pi^2 r^2} i_{\parallel}(\gamma), \tag{4}$$

and

$$J_u(\gamma) = \frac{\lambda^2}{8\pi^2 r^2} (i_{\perp} + i_{\parallel})_{(\gamma)}. \tag{5}$$

Here, r is the photometric distance and the subscript u identifies an unpolarized incident beam. These and all following equations are valid if $r >> \lambda$. More convenient than the dimensionless quantity J is the quantity

$$J'(\gamma) = r^2 J(\gamma) \quad cm^2 \tag{6}$$

which represents the intensity of light scattered per unit solid angle and per unit intensity of the incident beam in the direction γ. Equation (6) is all that is needed if the sphere is large enough to give a directly measurable J'. Only one instance is thus far known where light scattering measurements on a single microscopic sphere were successful[30]. Generally, only the effect produced by a reasonably large number of spheres per volume unit, N, is well measurable. Since

$$N = 6\pi^2/\alpha^3\lambda^3 V_t \quad cm^{-3} \tag{7}$$

where V_t is the optically effective (irradiated and observed) volume of the scattering system, it follows that the specific intensity of light scattered, per unit solid angle and unit intensity of the incident beam, by 1 cm^3 of the scattering system is

$$(I/I_0 \varphi)_{(\gamma)} = 3i(\gamma)/2\lambda\alpha^3 \quad cm^{-1} \tag{8}$$

where φ is the volume fraction of the spheres. Since

$$\alpha = \frac{D\pi n_2}{\lambda_0} = \frac{n_1}{\lambda_0}\left(\frac{6M\bar{V}\pi^2}{N_A}\right)^{1/3}, \tag{9}$$

where λ_0 is the vacuum wave length, and n_1 is the refractive index of the medium in which the spheres are dissolved, dispersed, or embedded, N_A is Avogadro's number, and V is the partial specific volume of the spheres. One can determine the diameter of a sphere, D, or its "molecular weight", M, by inserting in eq. (8) the experimental value of $(I/I_0\,\varphi)\,(\gamma)$ extrapolated to zero φ in order to exclude interference by multiple scattering.

On integrating the $J_{\parallel}(\gamma)$ and $J_{\perp}(\gamma)$ values over the surface of a sphere of unit radius and on taking one half of the sum, one obtains the total scattering cross section, R, of a sphere. It may be calculated more simply from the relation

$$R = \frac{\lambda^2}{2\pi} \sum_{n=1}^{\infty} \frac{|a_n|^2 + |b_n|^2}{2n+1} \quad cm^2 \qquad (10)$$

which also follows directly from the Mie theory. (For a definition of the symbols in Eq. (10) see e.g. ref. 31.)

This scattering cross section does not correspond to the geometrical cross section. Its value relative to that of the geometrical cross section, $r_s^2\,\pi$, i.e. the scattering coefficient,

$$K = \frac{2\sum}{\alpha^2} \qquad (11)$$

(where $\sum$ is an abbreviation for the summation in eq. (10)) oscillates with decreasing amplitude, as α increases, about a mean value of 2.0, as shown in Fig. 2 for $m = 1.20$*.

The quantity generally measured is neither R nor K but the relative loss in intensity of the incident beam on traversing a system containing N spheres

---

*For nontransparent, i.e. for strongly absorbing scatterers, the value of K obviously should be 1.0 as $\alpha \to \infty$. For transparent scatterers, considered here, the interference between primary and scattered wave in the forward direction results in a dissipation of energy equal to twice that dissipated by scattering itself.

per cm^3. The resultant coefficient of "apparent" absorption, generally denoted as turbidity

$$\tau = \frac{1}{x} \ln\left(\frac{I_0}{I}\right) = NR \quad cm^{-1} \tag{12}$$

where I_0 is the intensity of the incident beam, I the intensity of the beam emerging from the scattering system, and x is the path length of the scattering cell. Introducing eq. (7), one obtains the dimensionless quantity

$$\frac{\lambda\tau}{\varphi} = \frac{3\pi}{\alpha^3}\sum = \frac{6\pi^2 R}{\alpha^3\lambda^2} = \frac{3\pi}{2\alpha}K \tag{13}$$

The specific turbidity, $\frac{\tau}{\varphi}$, therefore gradually decreases, at constant wave length, to zero as α increases, after having traversed one single prominent maximum.

The quantities contained in the summation $\sum$, just like those contributing to i (eqs. (1) and (2)), depend in a very complicated fashion on α, m and β, where $\beta = m\alpha$. In contrast to this, the situation is rather simple on using the approximating theories considered in Fig. 1. Maintaining the symbolism used for the Mie-theory, one readily finds that in the case of the Rayleigh theory

$$i_\perp(\gamma) = \xi\alpha^6 \tag{14}$$

$$i_\parallel(\gamma) = \xi\alpha^6(1+\cos^2\gamma) \tag{15}$$

$$i_u(\gamma) = \frac{\xi}{2}\alpha^6(1+\cos^2\gamma) \tag{16}$$

where

$$\xi = \left[(m^2-1)/(m^2+2)\right]^2 \tag{17}$$

The Rayleigh-Gans theory yields

$$i_u(\gamma) = \frac{\xi}{2}\alpha^6(1+\cos^2\gamma)\,P(\alpha) \tag{18}$$

where the "interference" factor

$$P(\gamma) = 9\left[\sin(s_\gamma \alpha) - (s_\gamma \alpha)\cos(s_\gamma \alpha)\right]^2/(s_\gamma \alpha)^6 \tag{19}$$

and

$$s_\gamma = 2\sin(\gamma/2)$$

Since, except for limited α ranges (see Fig. 1), (m-1) must be very small

$$\xi = \underset{(m-1)\to 0}{\frac{(m^2-1)^2}{9}} \tag{20}$$

so that one may write

$$i_u(\gamma) = \left[(m^2-1)^2/9\right]\frac{\alpha^6}{2}(1+\cos^2\gamma)P(\gamma) \tag{18a}$$

which is the form of the equation actually given by Rayleigh. Both eqs. (18) and (18a) reduce, of course, to the simple Rayleigh equation (16) if $\gamma = 180^\circ$ where $P = 1.0$.

The classical definition of the interference factor given in eq. (19) is rarely being used at present in favor of alternate equivalent formulations. It should also be noted that the value of P has been evaluated not only for spheres, but also for rods, disks and random coils[32].

The Stevenson equation finally gives*

$$i_1(\gamma) = \frac{\xi}{2}\alpha^6 + 2\sqrt{\xi}\left[\frac{2}{5}\xi\left(\frac{m^2-2}{m^2-1}\right) - \frac{1}{15}\frac{(m^2-1)(m^2+4)}{2m^2+3}\cos\gamma\right]\alpha^8 \tag{21}$$

---

*Equations (21), (22), (23) and (24) not developed explicitly in Ref. 7 were kindly provided for this publication by Professor A. F. Stevenson.

$$i_{11}(\delta) = \tfrac{1}{2}\alpha^6 \cos^2\gamma - 2\cos\gamma\sqrt{\tfrac{1}{2}}\left[\frac{m^2-1}{30} - \frac{3}{5}\tfrac{1}{2}\left(\frac{m^2-2}{m^2-1}\right)\cos\gamma + \frac{(m^2-1)}{(6\,12\,m^2+3)}\cos 2\gamma\right]\alpha^8 \tag{22}$$

which simplifies, for $\gamma = 90^0$, to

$$i_{\perp 90} = 2\,i_{u 90} = \tfrac{1}{2}\alpha^6\left[1 + \frac{6}{5}\,\frac{m^2-2}{m^2+2}\,\alpha^2\right] \tag{23}$$

$$i_{11 90} = 0 \tag{24}$$

IV Survey of Experimental Methods

The purpose of scattering measurements on systems containing spheres of uniform size is generally the determination of the diameter, D, or the weight, M, of a sphere. If the spheres do not all have the same size, then evaluation of the size distribution is an additional problem which one may wish to solve by scattering measurements. The principal experimental procedures available for a determination of D or M are enumerated in Table II. Each procedure is evaluated critically as to its merits and shortcomings to the extend sufficient information is available. The evaluations given are based predominately on the experience gained in the writer's laboratory. The remainder of this article is concerned primarily with an elaboration of the information given in Table II. In view of the large amount of experimental work published in this field and the restricted size of this essay, reference can be made only to a limited number of the worthwhile investigations published by various authors.

1. Turbidity Measurements

Turbidity measurements are very attractive because the technique is relatively simple, the particle sizes derived are absolute sizes, and precision and accuracy can be scaled so high that errors in particle diameter need not exceed 2%[35]. As seen in Fig. 3[33,34], the results, are in general,

bi-valued. Measurements at two wave lengths allow one, however, to decide very quickly as to whether one operates on the ascending or descending branch of the relatively simple $(\frac{\tau}{c})_\lambda$ vs α -curve. If m is large (> 1.25) secondary oscillations introduce problems in single valuedness at α -values > 10*. One feature that requires extremely careful attention is the importance of the solid angle of the incident beam, and particularly, of the scattered beam. Unless it is sufficiently small, the results obtained may be quite erroneous [34]. Another disadvantage is that a precise knowledge of the concentration of the scattering material is mandatory if useful results are to be obtained in monochromatic light. On the other hand, extrapolation of $(\frac{\tau}{c})$ or $(\frac{\tau}{\varphi})$ to zero concentration is very simple, since the plot of such data against c or φ gives at low concentration a rigorously straight line[35], which has zero slope if the heat of dispersion or of solution is zero**. As regards the speed of measurements, turbidity measurements are most likely the fastest possible scattering measurements, considering the time elapsed from the filling of the scattering cell until the particle size evaluated from turbidity tables[31,33] is recorded. The α -range accessible to turbidity measurements is restricted at both very low and very high α-values, unless in both instances very long cells are employed. Otherwise the precision is rather poor if α is $< \sim 0.3$ and $> \sim 50$ since the transmittancy is then far too high at the mandatory low concentrations***.

---

*In order to provide a simple correlation between α and particle diameter for those working with visible light, it may be stated that $\alpha = 1.0$ corresponds to a particle diameter of 130.302 mμ, if $\lambda_o = 5460.73$ Å and if the medium is water at 25.000°C.

**The quantity c represents the concentration in g/100g.

***With very long cells, on the other hand, one may go considerably below this limiting α -value as documented by the quite satisfactory molecular weight determination of egg albumin from the turbidity in 18 cm cells[36] (M = 47,000 ± 1500 as compared to 44,000, the most recent literature data obtained from sedimentation and diffusion).

For further information on turbidity measurements see also references 37 and 38.

2. Light Scattering at $\vartheta = 90^{\circ}$

Light scattering measurements at an angle of 90° with respect to the incident beam have for many years been the favored method in connection with molecular weight determinations in macromolecular solutions. In contradistinction to turbidity measurements, there exists no lower limit for α. Even molecular weights as low as a few thousand can, in principle, be determined quite accurately. As shown in Fig. 4[39], 90° measurements have the disadvantage in that the results are multivalued unless the approximate size range involved is a priori known. As long as one is certain that $\alpha < 3$ results are merely bivalued so that measurements at two wave lengths can then resolve the problem. (By using visible light, this corresonds to an upper value for the particle diameter of approximately 400 m μ.) As in turbidity measurements, the results in order to be reliable require that the concentration be known as accurately as possible. Furthermore, the solid angle should be as small as is compatible with the requirement of a reasonably large response of the phototube. It should preferably not exceed 4×10^{-4} steradian[40] or one should extrapolate the experimental data, referred to unit solid angle, to zero solid angle[40]. One major disadvantage compared to turbidity measurements is the fact that the data obtained by experimentation have to be multiplied by an instrument constant* before they can be compared to theoretical data. If the instrument is very well constructed, one may derive the absolute value of the instrument constant which eliminates the empirical feature involved in calibrations. However, the best that one could accomplish

*For a comprehensive review of the problem of calibration see Ref. 41.

in this direction thus far is a theoretical constant differing by not more than 15% from that obtained by calibration[40]. (There is no doubt that this uncertainty can be reduced still further.) An additional feature which complicates 90°-measurements is the fact that for certain α-values extrapolation of $I/I_o c$ to zero concentration is rather difficult on account of pronounced changes in slope at even very low c[40]. These changes are more pronounced the larger the solid angle of the scattered beam, so that only very drastic reduction of the solid angle can resolve this problem. While it therefore appears that turbidity measurements deserve preference over 90° measurements, provided that α- and m-values involved allow one to make precise turbidity measurements, it is necessary to make one important reservation: the rapid change of scattering with α, apparent in Fig. 4, makes 90°-measurements an incomparably more sensitive tool for detecting relatively small changes or small differences in size, particularly in those α-ranges near the turbidity maximum, where the turbidity changes relatively little with α. It also has been established[40] that accuracy and precision of measurements conducted properly with the proper kind of apparatus are about the same as for turbidity measurements.

3. Scattering Ratio, Polarization Ratio and Depolarization

Most of the drawbacks encountered with measurements of the intensity of light scattered from an unpolarized (or polarized) beam at 90° with respect to the incident beam, can be eliminated by measuring rather intensity ratios. There are two possibilities at constant wave length. The first one consists of making two consecutive measurements of the total intensity of light scattered from a linearly polarized incident beam whose electric vector first vibrates

---

*The considerably less good agreement actually reported in the publication referred to resulted from an error in calculation.

parallel and subsequently perpendicular to the plane of observation. The ratio of the two quantities $I_{//}/I_o$ and $I_{\perp}/I_o$ measured in succession, i.e. $I_{//}/I_{\perp}$ is identical with $i_{//}/i_{\perp}$. It has been designated as "scattering ratio"[43]. The second possibility consists of using an unpolarized incident beam and of determining with the aid of an analysing prism interposed between scattering cell and observer, first the intensity of scattered light vibrating in the plane of observation and, subsequently, of that vibrating perpendicular to the plane of observation. This is the classical procedure in depolarization measurements. It has been used extensively by LaMer[37] and Kerker[42], particularly in connection with size determinations in sulfur sols. Since these authors used the ratio $I_{//}/I_{\perp}$ (where the subscripts have now a different meaning from that of above) also at angles other than 90°, they designated it as "polarization ratio". In the case of spheres, measurements of the scattering ratio and of the polarization ratio (de polarization) give identical results. Therefore, the results of recent systematic theoretical[44] and experimental[45] investigations of the scattering ratio apply also to the alternate effect.

One of the most obvious advantages of the ratio $I_{//}/I_{\perp}$ as compared to $I/I_o c$ is that the concentration does not directly enter in the numerical results. Moreover, on extrapolating this ratio to zero concentration, one will find that, with very few exceptions, its slope is constant in the range of low concentration[45]. In addition, the effect of the solid angle is drastically reduced since it affects, in a first approximation, both denominator and numerator similarly unless a scattering maximum or minimum is located at or very near 90°[45]. Finally, the data obtained are absolute data which do not require use of an instrument constant unless the photosensitive area of the photocell is anisotropic or unless there are some more obvious shortcomings in the optics of the instrument used. It is

therefore not surprising that the particle size determinations by means of scattering ratio (or polarization ratio) measurements are both highly precise and accurate. Table III shows the good agreement of particle diameters determined from the scattering ratio (D_o) and by electron microscopy (D_e) respectively[45]. The only two limitations to the use of the scattering ratio are: 1) as in the preceding method (2) results on particle size obtained at a single wave length are multivalued; 2) in contradistinction to the preceding method, there is a lower limit for α below which the scattering ratio cannot be used. The value of $i_{//}$ is zero at α-values smaller than those given in Table I and it is large enough to allow precise data of $I_{//}/I_{\perp}$ only if $\alpha \geq 2.0$. The most advantageous α-ranges for the experimental use of the scattering ratio and their dependence on m follow easily from available detailed graphs and tables[44].

4. Dissymmetry

Figure 5 shows three characteristic phase in the changes occurring in the radiation diagram of spheres as α increases. Diagram A is representative of pure dipolar Rayleigh scattering characterized by perfect symmetry of the radiation diagram. Diagram B shows how the radiation diagram becomes dissymmetrical once the dimensions of the sphere are no longer small compared to the wave length. More light is being scattered at angles $\gamma > 90^\circ$ than at angles $\gamma < 90^\circ$. This effect, originally called Mie-effect because it was discovered both theoretically and experimentally (through experiments by Steubing) by Mie, is nowadays generally referred to as dissymmetry. It is clear from diagram B in Fig. 5 that the ratio of the intensity of light scattered at $\gamma = 45^\circ$ to that scattered at $\gamma = 135^\circ$, i.e. I_{45}/I_{135} should provide a useful method for particle size determinations. Considering a median m-value of 1.20, it was

found that this ratio should in fact be particularly useful in the range $0.4 < \alpha < 2$[43]. Here, the ratio decreases about 100 fold with rising α, i.e. it is here extremely sensitive to changes in particle size. It is on account of this high sensitivity to particle dimensions (and to particle shape) in the lower α -range immediately following the Rayleigh range that dissymmetry measurements have assumed an outstanding role in determination of molecular weights and molecular shapes in macromolecular chemistry and physics[32]. There, one rarely exceeds an α-value of 0.4 - 0.6 and therefore is virtually free from the risk of multivaluedness of results. The problem of multivaluedness is here the same as with the two preceding methods. One might remove it by using as an additional argument $(I_{\parallel 45}/I_{\parallel 135})$ or/and $(I_{\parallel}/I_{\perp})_{45}$ and $(I_{\parallel}/I_{\perp})_{135}$[42,43]. At α -values > 2, no reason can be seen why dissymmetry measurements should be perferred to those of the scattering ratio (depolarization) at 90°, or at other angles, or to other methods to follow below.

5. Forward and Backward Scattering

Scattering in the forward direction (direction of the primary beam) and backward direction is in special cases of major interest. Considering first back scattering, Fig. 5, reproduced from a recent theoretical study[46], shows that the maxima and minima of i follow each other much faster with increasing α than at 90° (Fig. 4) and that the first maximum occurs at an α -value as low as 1.45 if m = 1.20. There is certainly no interest in determining particle sizes or molecular weights by extrapolating angular data to $\gamma = 0°$. However, the theoretical data available[18,19] are of major interest for the theoretical treatment of such problems as visibility through illuminated clouds and smokes as a function of particle size[47]. In addition, on taking into account multiple

scattering, these data should allow one to approach the problem of optimum grain size in paints and in light and radar reflecting devices in a non-empirical, fundamental way.

Forward scattering, in considerable contrast to back scattering, exhibits no maximum or minimum at α-values < 15 as long as $m \leq 1.20$[48]. This, again, applies to i*. Particle sizes obtained from forward scattering, by means of Zimm plots[11], are therefore single valued within relatively large ranges of values of the variables α and m. An additional attractive feature is that one may at sufficiently small m-values use the simple Rayleigh equation (see eq. (16)) without making a major error in particle diameter even at α-values > 10**. From detailed data given elsewhere[48], one arrives at the following approximate α-values leading to an error in particle diameter in excess of 5% (in brackets: in excess of22%) on using eq. (16) in connecting with forward scattering.

m	α
1.05	>15 (>2)
1.10	12 (<1)
1.15	$\leq$ 2 (<1)

Except for these two advantages, there is no incentive to use forward scattering in preference to the experimentally simpler scattering ratio or turbidity measurements.

6. Angular Scanning

As soon as α is large enough so that the first scattering maximum is generated at $\varphi = 0^\circ$ (Fig. 6), an intriguing method of particle size deter-

---

*It may be recalled that the maxima for $(I/I_0 c)$ occur, of course, at α-values appreciably smaller than those of i. Those of I/I_0 occur at the same α as those of i if λ is kept constant.

**The equation actually involved is the R-G-D- equation (18). Since $P = 1$, if $\varphi = 180^\circ$, it reduces for this angle to eq. (16).

mination begins to become possible. With a further increase in α, the first maximum moves forward and a second maximum is being generated at $\gamma = 0^{\circ}$. Thus, the radiation diagram soon begins to exhibit a series of maxima and minima as shown for a limited number of small γ-values in diagram C of Fig. 5. It is therefore possible to determine particle sizes simply by scanning, i.e. by determining the angular location of a maximum or minimum or of maxima and/or minima. Dandliker was the first to give more than cursory attention to this possibility[49]. A detailed examination of the theoretical aspects and potentialities of this method[28] shows that an unequivocally single-valued answer on particle size can be obtained on determining both the angular location and angular separation of an intensity maximum and of an adjacent intensity minimum. Outstanding other advantages of the method are: a) the concentration has a relatively small effect upon the angular location of maxima and minima[50,51]; b) the accuracy in the particle diameters obtained is very high if a sufficiently small solid angle is used[51]; c) there is no need for an instrument constant; d) the sensitivity of the angular location of maxima and minima to changes in particle sizes is very high at angles $< 90^{\circ}$, more so the closer one approaches to $\gamma = 0^{\circ}$. There is therefore an advantage in working at small γ-values[28]. (Several authors have used and advocate the use of maxima or minima close to the forward direction. By doing this, one loses the two outstanding advantages of the scanning method - high sensitivity to changes in α and accuracy of the α-values derived.); e) interpolation of α-values from theoretical data (e.g. ref 18) is relatively secure, with the exception of high orders of maxima and minima, the α-values associated with an intensity maximum or minimum vary above $\gamma = 45^{\circ}$ linearly with $\left[2 \cos (\gamma/2)\right]^{-1}$ and nearly linearly with it if $\gamma < 45^{\circ}$ for

higher order maxima and minima*. Disadvantages of the scanning method are: 1) The results depend very strongly on solid angle, more so the more numerous the maxima and minima are[51]. 2) The determination of a scan requires far more time than most of the other procedures, unless the need for manual operation is eliminated by automation.

7. Spectra

Spectra of the light scattering quantities are of interest for several reasons. First of all, they allow one by normalization to eliminate the direct contribution of errors in concentration determinations to the accuracy of particle sizes to be derived from $\left(\frac{\tau}{c}\right)$ or $(I/I_0c)_\gamma$. For this purpose, one simply uses as a criterion of particle size coincidence of a normalized section of the experimental turbidity spectrum or of the scattering spectrum at a given angle of γ with a normalized section of the corresponding theoretical spectrum[52]. The same purpose is served by considering instead of a spectrum of finite width rather a differential spectrum. This is done in particle size determinations by means of the "wave length exponent"[53,54,38]. The latter is of particular interest if the objective of the measurement is speed without need of high accuracy, the former is indicated if high accuracy is the prime objective and time requirement is of secondary consideration.

The second possible motivation for the study of spectra is elimination of multivalued answers on particle size, which arise on using several of the methods discussed above (2, 3, and 4). There is no instance where use of spectra (if necessary of two quantities) cannot resolve the problem of multivaluedness.

Thirdly, spectra observed with incident polychromatic (e.g. white)

---

*If $m > 1.20$, these simple relationships gradually become invalid and the movement of the maxima and minima with increase in α may become quite complicated.

light rather than those obtained by systematic variation of wave length in scattering experiments may provide an extremely convenient, although not highly accurate, method of rapid particle size determinations. Thus, the turbidity spectrum exhibited by the setting sun could, depending on the particular hue within the limits of light orange and deep red, give information on the amount and/or approximate size of dust in the atmosphere. Of particular interest, however, are the colors which one can observe in the light scattered laterally by systems which contain particles of nearly uniform size. These colors which vary on varying the angle of observation systematically between 0° and 180° were discovered by Ray[55], but they were systematically studied first and foremost by LaMer[37,56] who designated the m as "Higher Order Tyndall Spectra" (HOTS). In LaMer's method, one determines the angle γ at which a characteristic color band (a "red band" is preferred) is observed. By calibration or by using composite angular Mie data, particle sizes follow immediately. These colors are, of course, a consequence of the fact that the lateral scattering maxima and minima (see Fig. 5 c) move, at constant particle size, towards the forward direction as the wavelength decreases. This is shown on one example[51] in Fig. 7. Consequently, a distinct color will be observed at that angle γ at which scattering reaches either a maximal or minimal value at a wave length contained within the visible spectrum. This also is shown in Fig. 7 (dashed curve). While particle sizes determined by means of HOTS can, of course, not possibly compete in accuracy with those obtained in monochromatic light from the location of angular maxima and minima, the method is very elegant and very simple and, therefore, has distinct advantages whenever speed in the determination of approximate particle sizes is essential, and whenever the system is sufficiently monodisperse to make the method applicable.

The fourth and last reason which makes the study of light scattering spectra attractive is their paramount importance in determining size distribution curves. Extensive scrutiny of the scattering effects most suited for a determination of size distribution curves led to the selection of the spectra of the scattering ratio at $\gamma = 90^{\circ}$ as the primary criterion[57] and of the trubidity spectra as an auxiliary criterion[58,*]. Figure 8 shows the theoretical effect of increasing heterodispersion upon the amplitude in the oscillation of the scattering ratio using a particular type of distribution curve picked for the study of emulsions[57]. (The Basic effect of heterodispersion, illustrated in Fig. 8, is, of course, independent of the type of distribution assumed.) Figure 9, finally shows the remarkably high resolving power of scattering spectra in determining size distribution curves. This figure[52] gives the size distribution curve of a latex generally referred to as "monodisperse".

While the study of turbidity and scattering spectra possesses, therefore, many advantages over the study of these phenomena in monochromatic light, there are, of course, several disadvantages. One is the fact that the experimental setup is more complicated except for the very simple method of HOTS observation. Another, far more serious disadvantage, is the importance of dispersion corrections which have been neglected by various authors but can be neglected only if (a) rigorously accurate sizes or size distributions are not aimed at or if (b) the dispersion of the scattering material and of the dispersing medium or solvent are nearly the same.

---

*Undoubtedly the angular variation of scattering also can provide a powerful tool. In order to make if applicable, angular scattering functions are now being extended to α -values > 7.0 (see ref. 18).

TABLE I

LIMIT OF VALIDITY OF THE RAYLEIGH EQUATION

The α-values given are the upper limit, at the respective m, beyond which the Rayleigh specific turbidity equation (13) gives α-values in error by more than 2%*.

m	α
1.05	0.23
1.10	0.25
1.15	0.28
1.20	0.31
1.25	0.35
1.30	0.42

* This Table is reproduced from the table given in Ref. 6.

TABLE II

ADVANTAGES (+) AND DISADVANTAGES (-) OF VARIOUS LIGHT SCATTERING METHODS

	1	2	3	4	5	6	7	8
1. Turbidity	+	+	-	-	+	+	+	> 0.3 < 50
2. Scattering at $\gamma = 90^\circ$	-	-	-	-	$\pm$	+	+	NR
3. State of Polarisation at 90°	+	-	+	+	+	+	+	> 2.0
4. Dissymmetry	+	-		+		+	+	> 0.4
5. Forward Scattering ($\gamma = 180^\circ$)	-	+		+	$\pm$	-		NR
6. Angular Scanning	+	+	-	+	+	-	+	> 1.5
7. Spectra of 1, 2, 3, 6	+	+	$\pm$	+	$\pm$	-	+	

Code

1: Particle size derived is absolute (+); requires use of instrument constant (-).

2: Particle size derived is single valued (+); multivalued (-).

3: Solid angle of scattered beam affects result very little (+); very much (-).

4: Exact knowledge of concentration is not important (+); very important (-).

5: Extrapolation of affect to zero concentration is easy (straight limiting slope) (+); difficult (curves) (-).

6: Execution of experiment requires little time (+); much time (-).

7: Precision of data high (+); low (-).

8: α -Range accessible for quantitative work if $m = 1.20$ (both lower and and upper limits decrease with increasing m).

NR: No Restriction

$\pm$: Depends on α -values whether + or -.

TABLE III

COMPARISON OF PARTICLE DIAMETERS FROM SCATTERING RATIO AND ELECTRON MICROSCOPY

(Polyvinyltoluene) (m = 1.188)

Sample No.	σ_o	D_o mu	D_e mu	% Deviation
42	0 014	163	163	+
23	0.17	307	315	-2.5
2013	—**	-	381	—
43B	0.37	417	421*	-1.0
43B	0.21	431	445	-3.1
44A	0.092	507	492	3.0
43C	0.10	514	528*	-2.7
43C	0.21	554	558	-0.7
43C	0.43	685	699*	-2.0
44B	0.26 - 0.30	562 - 569	587	-3.1 - 4.3
44B	—**	-	620	—
44C	0.18	772	780*	-1.0
44C	0.29	812	824	-1.5

*Normalized Particle Diameters

**Extrapolation to σ_o unsafe

LEGENDS TO FIGURES

Figure 1 Error Contour Chart

Contour lines indicate 5% deviation of $(\lambda\tau/c)$ -values relative to value derived from Mie-theory.

Figure 2 Scattering Coefficient for m = 1.20

Figure 3 Variation of τ/c of Spheres with α

Vacuum wave length λ_0 = 5460.73 A; medium: water at 25.000°C; concentration c in g/100 g.

Figure 4 Variation of Specific 90° Scattering of Spheres with α and m

Total scattering from an unpolarized incident beam, λ_0 = 5460.73 A; medium: water at 25.000°C.

Figure 5 Scattering in the Backward Direction ($\vartheta = 0°$)

Figure 6 Lateral Maxima and Minima at Various Wave Lengths and Ratio of Blue/Yellow Intensities

Numbers on fully drawn curves indicate factor by which scattered intensities relative to intensity of incident were multiplied in order to obtain normalized intensity (1.0) at minimum. Dashed Curve: Blue/Yellow intensity ratio (right ordinate).

Figure 7 Theoretical Variation of Maxima and Minima of Scattering Ratio (Depolarization) with Increase in Width of the Size Distribution Curve as Expressed by Increasing q_R - Values

Increase in q_R means an increase in the width of the distribution curve. (For further explanations, see Stevenson, Heller and Wallach (Ref. 57)

Figure 8 Size Distribution of a Monodisperse Polyvinyltoluene Latex as Determined by Light Scattering and by Electronmicroscopy

The quantity C is proportional to the number of particles of a given radius r.

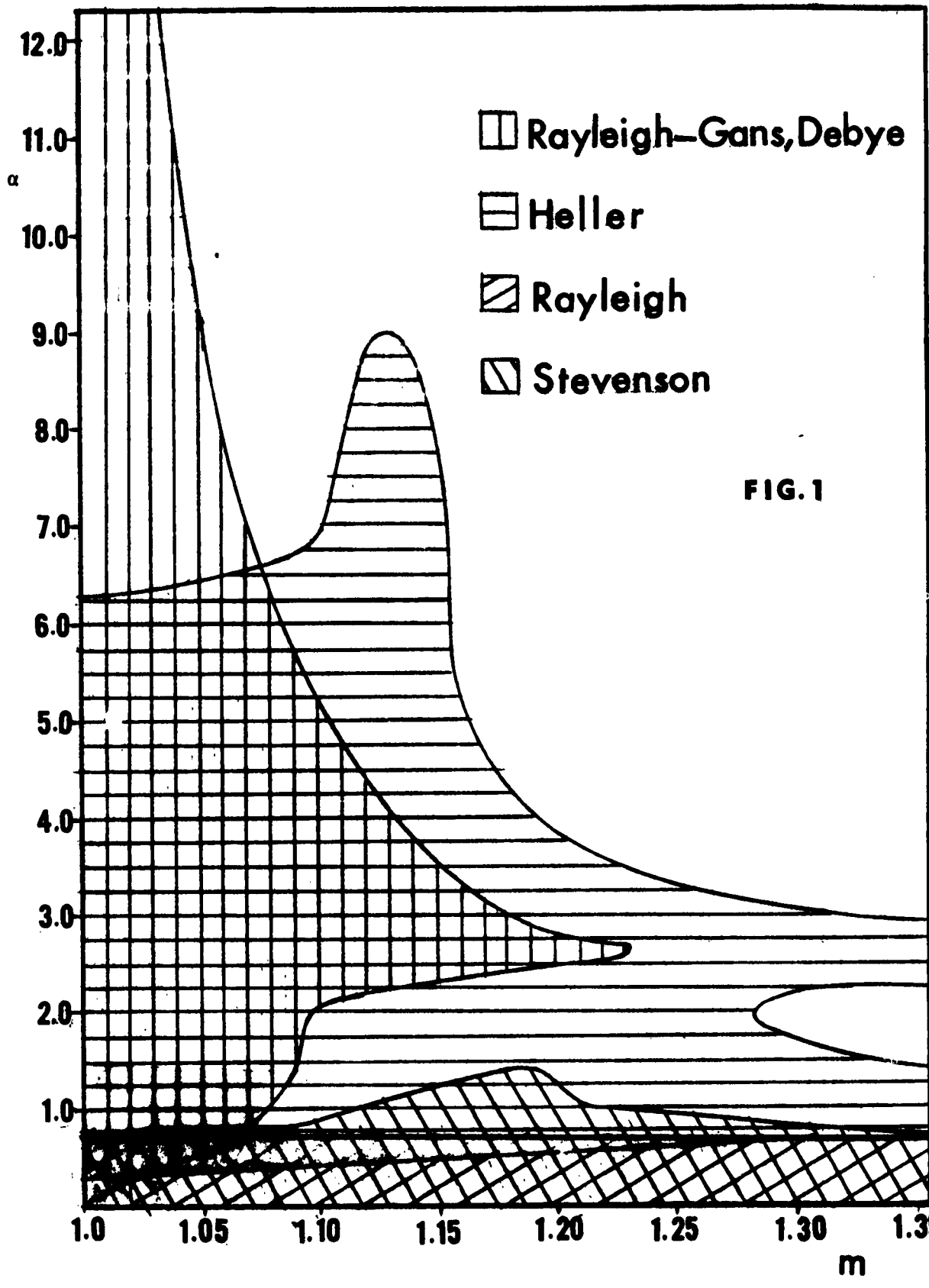
Rayleigh–Gans, Debye
Heller
Rayleigh
Stevenson
α
12.0
11.0
10.0
9.0
8.0
7.0
6.0
5.0
4.0
3.0
2.0
1.0
1.0
1.05
1.10
1.15
1.20
1.25
1.30
1.35
m

FIG. 1

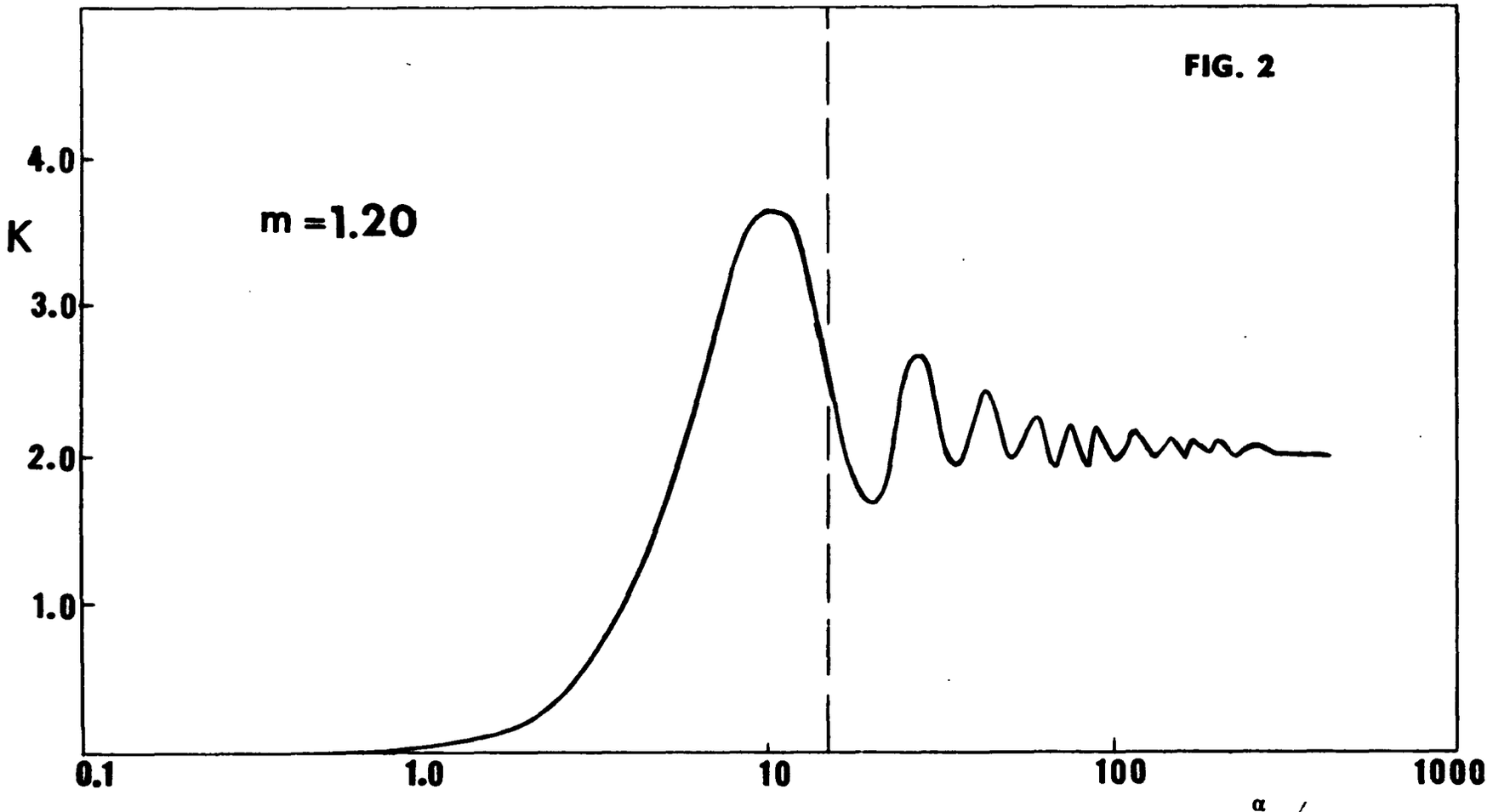
FIG. 2
4.0
K
m =1.20
3.0
2.0
1.0
0.1
1.0
10
100
1000
α

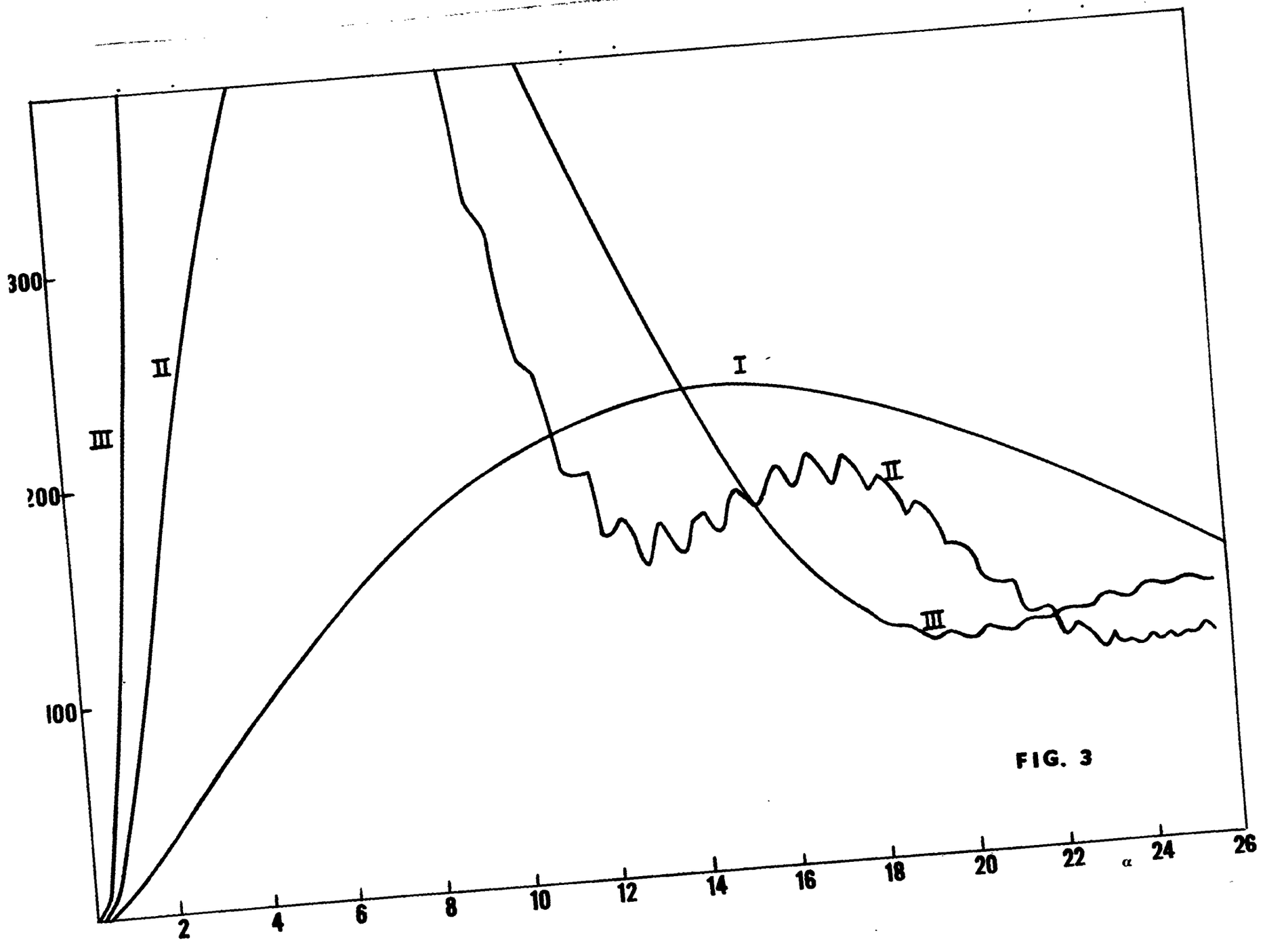

FIG. 3

FIG. 3

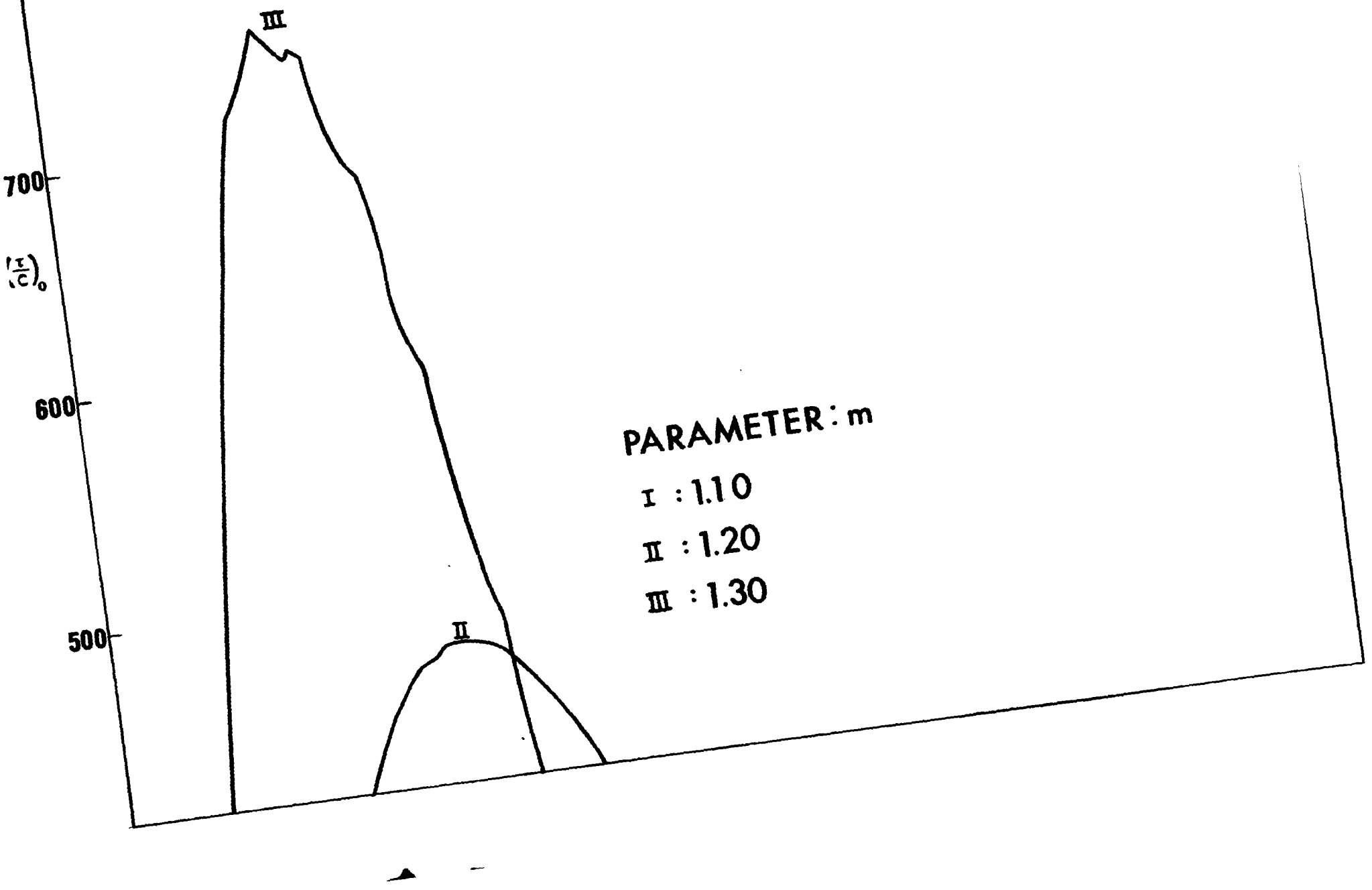

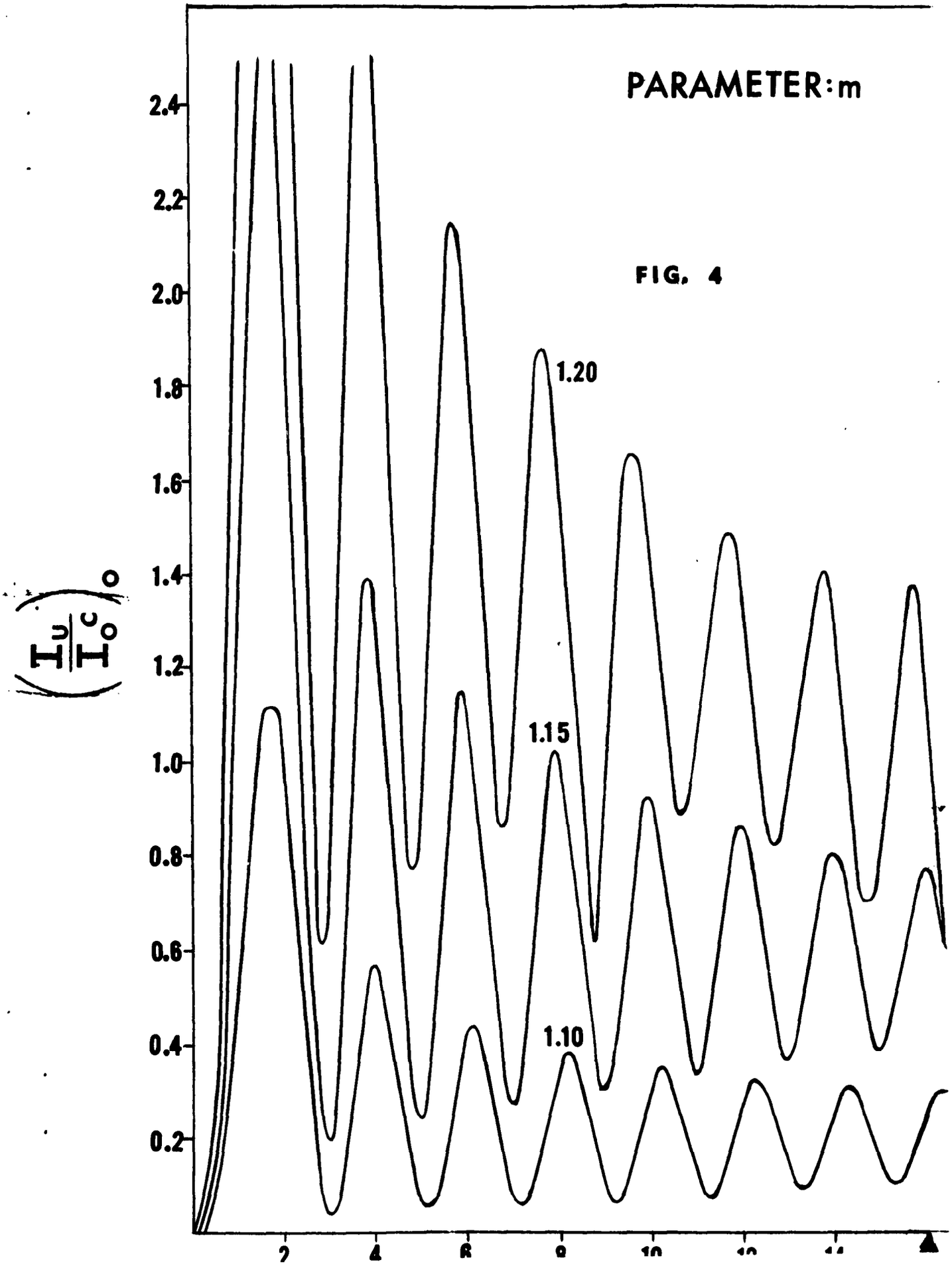
PARAMETER: m
FIG. 4
$\left(\frac{H_u}{H_{oc}}\right)_o$
2.4
2.2
2.0
1.8
1.6
1.4
1.2
1.0
0.8
0.6
0.4
0.2
1.20
1.15
1.10
2
4
6
8
10

FIG. 4

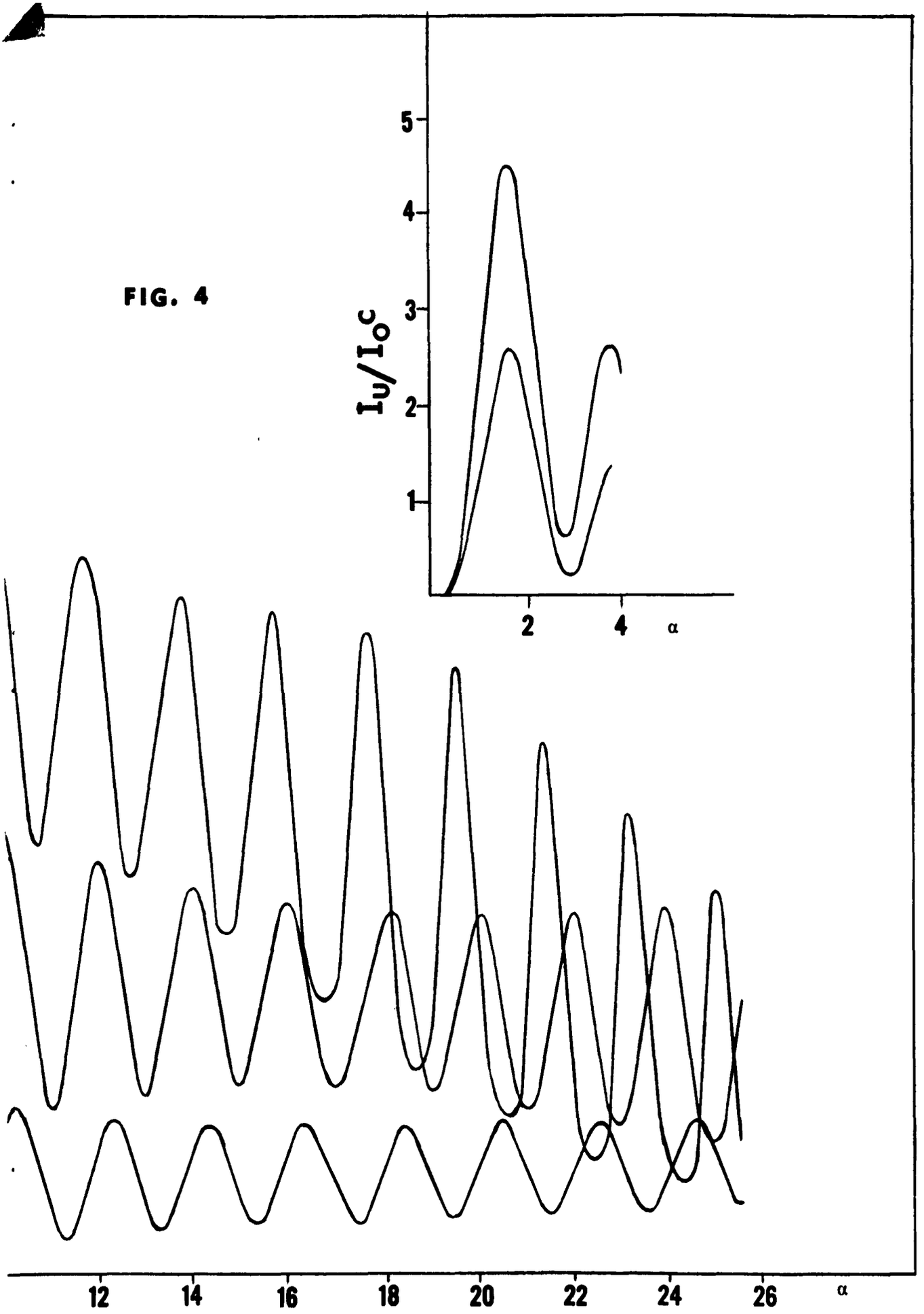

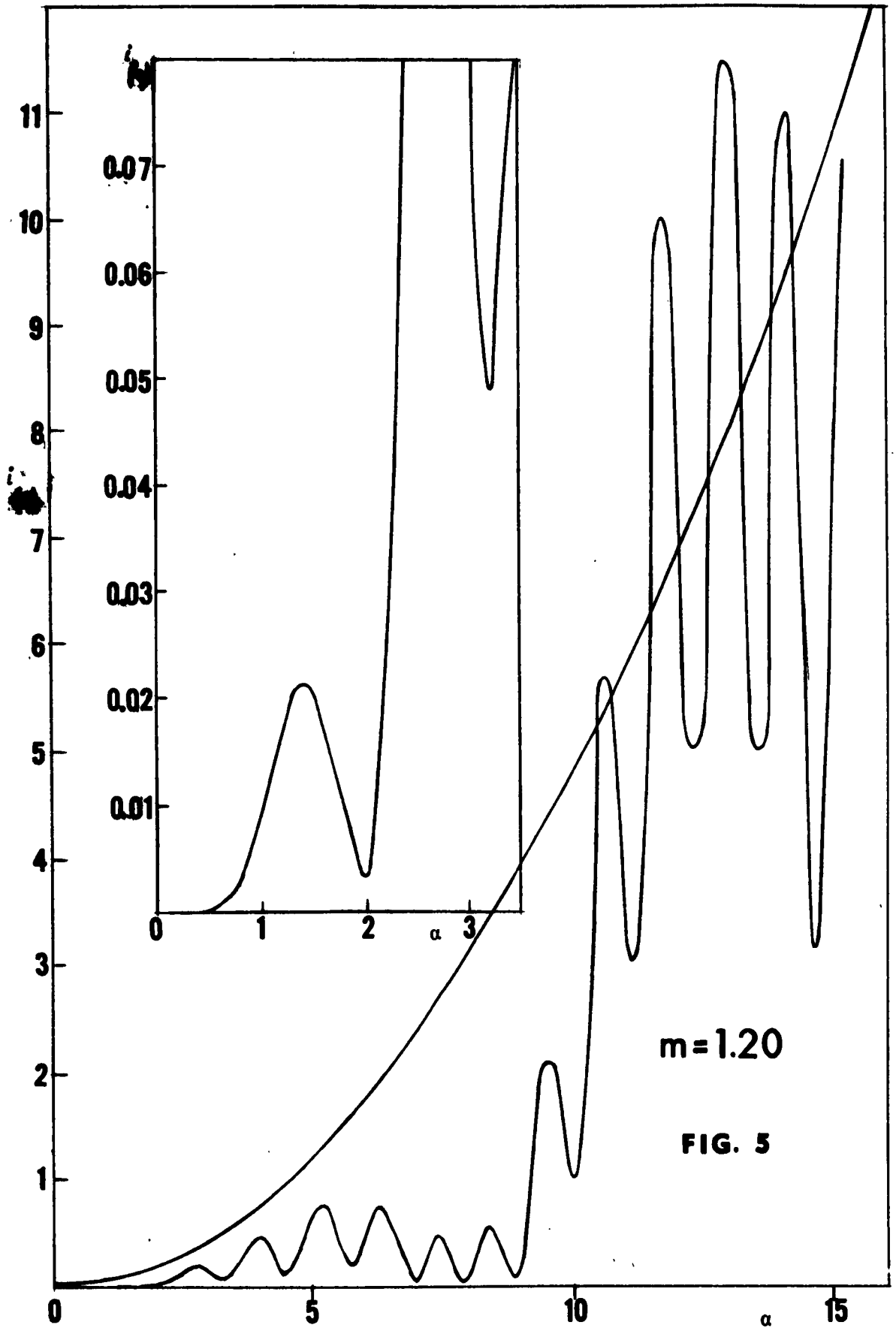
11
10
9
8
7
6
5
4
3
2
1
0
5
10
15
α
0.07
0.06
0.05
0.04
0.03
0.02
0.01
0
1
2
α
3
m=1.20

FIG. 5

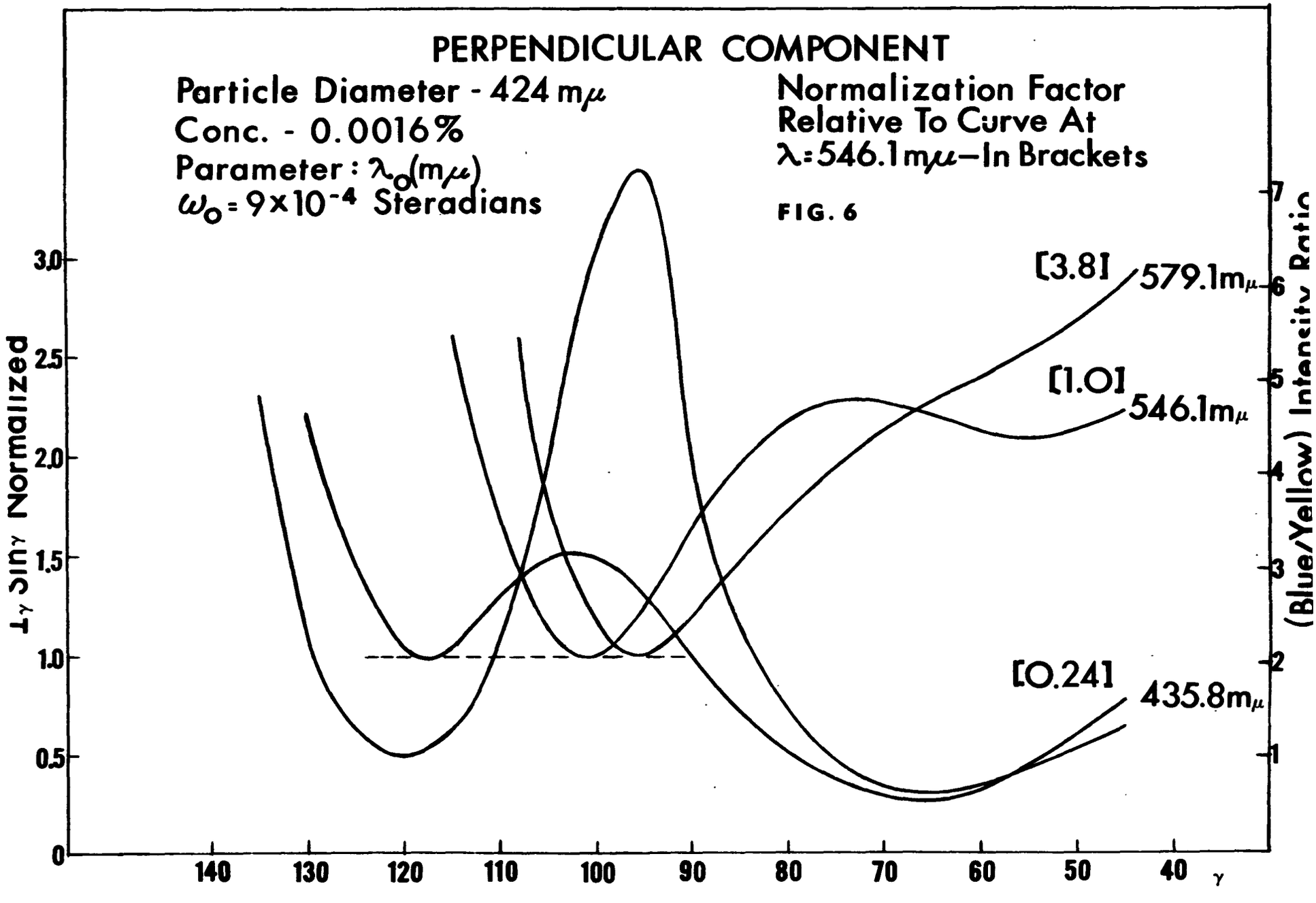
PERPENDICULAR COMPONENT
Particle Diameter - 424 mμ
Conc. - 0.0016%
Parameter : λo(mμ)
ωo = 9×10⁻⁴ Steradians
Normalization Factor
Relative To Curve At
λ=546.1mμ—In Brackets
FIG. 6
[3.8] 579.1mμ
[1.0] 546.1mμ
[0.24] 435.8mμ
I⊥γ Sinγ Normalized
(Blue/Yellow) Intensity Ratio
3.0
2.5
2.0
1.5
1.0
0.5
0
7
6
5
4
3
2
1
140
130
120
110
100
90
80
70
60
50
40
γ

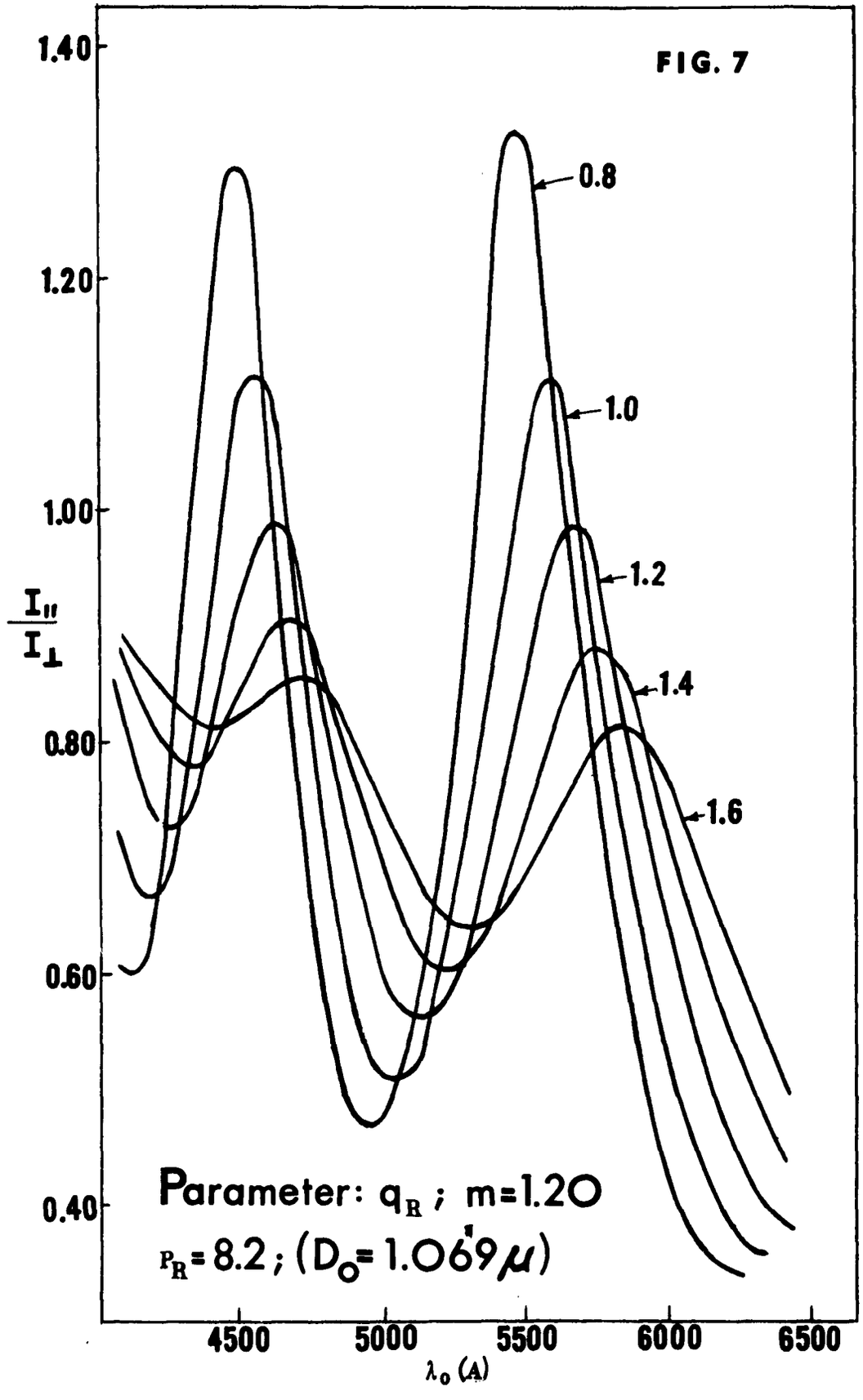
FIG. 7
1.40
1.20
1.00
0.80
0.60
0.40
$\frac{I_{\parallel}}{I_{\perp}}$
0.8
1.0
1.2
1.4
1.6
Parameter: q_R ; m=1.20
P_R = 8.2 ; (D_o = 1.069 μ)
4500
5000
5500
6000
6500
λ_o (A)

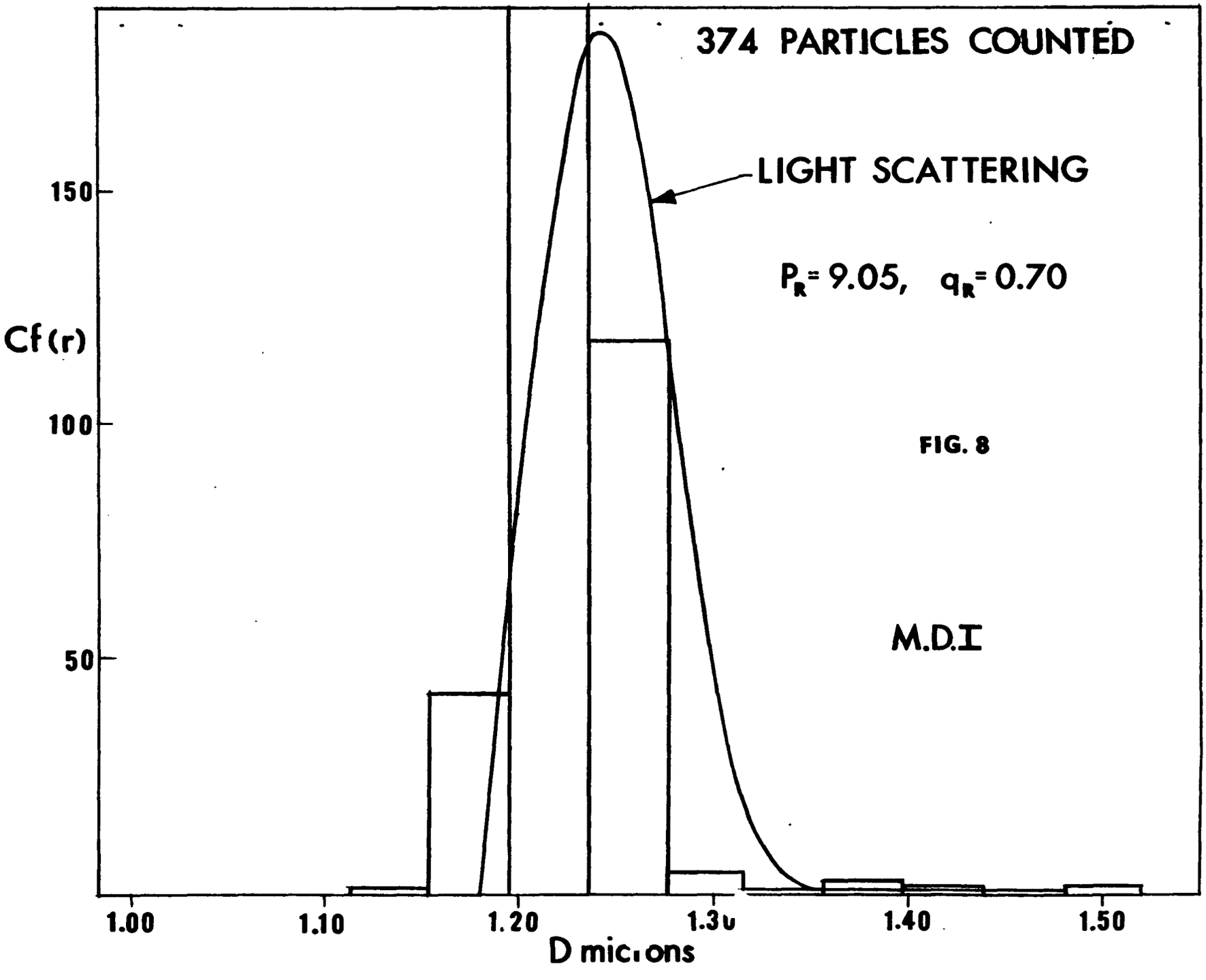
374 PARTICLES COUNTED
LIGHT SCATTERING
P_R= 9.05, q_R= 0.70
M.D.I
Cf(r)
150
100
50
1.00
1.10
1.20
1.30
1.40
1.50
D microns

FIG. 8

BIBLIOGRAPHY

1. Lord Rayleigh, Phil. Mag., 47, 375 (1899); 44. 28 (1897); 12, 81 (1881); 41, 107, 274, 447 (1871).

2. For quite comprehensive review of this earlier period see: a) R. Gans, in Handbuch der Experimental Physik, Vol. 19; Akademische Verlagsgesellschaft Leipzig (1928), p. 361. b) H. A. Stuart, in Hand- und Jahrbuch der Chemischen Physik, Vol. 8, Part 2, p. 1; Akademische Verlagsgesellschaft, Leipzig, (1936).

3. See for instance: P. Debye, various reports to the Office of Rubber Reserve, 1943 - 1946, issued from Cornell University; W. Heller, various reports to the Office of Rubber Reserve, 1943 - 1945, issued from University of Chicago; V. K. LaMer, various reports to OSRD since 1943, issued from Columbia University.

4. G. Mie, Am. Physik, 25, 377 (1908).

5. P. Debye, J. Applied Physics, 15, 338 (1944).

6. W. Heller, Rec. Chem. Progress, 20, 209 (1959).

7. A. F. Stevenson, J. Applied Physics, 24, 1143 (1953).

8. Lord Rayleigh, Proc. Roy. Soc. (London), A 84, 25 (1911); A 90, 219 (1914).

9. R. Gans, Am. Physik, 76, 29 (1925).

10. See P. Debye and Henke, Fortschr. Roentgenforsch., 2, 1 (1931). The theory developed in this paper applies to X-rays, but it is essentially the same as that suggested by Debye for light scattering. No detailed publication by Debye is available on this aspect.

11. B. H. Zimm, J. Chem. Phys., 16, 1093 (1948).

12. These limitations in α and n were analyzed in this laboratory by M. Nakagaki and will be the subject of a forthcoming publication.

13. W. Heller, J. Chem. Phys., 26, 1258 (1957).

14. A more detailed analysis of contour charts for these theories, using also angular scattering data, will be given in a separate publication in the near future.

14a. M. Nakagaki and W. Heller, J. Applied Physics, 27, 975 (1956); W. Heller and T. L. Pugh, J. Colloid Sci., 12, 294 (1957); B. H. Zimm and W. B. Dandliker, J. Phys. Chem., 58, 644 (1954).

15. H. Blumer, Zeitschr. f Physik, 32, 119 (1925); 38, 304, 920 (1926); 39, 195 (1926). See also the list of other early computations on pages 167 and 168 of Reference 24.

16. A. N. Lowan, Tables of Scattering Functions for Spherical Particles, Natl. Bureau of Standards (1948).

17. R. O. Gumprecht and C. M. Sliepcevich, Light Scattering Function for Spherical Particles; Engineering Research Institute, University of Michigan, Ann Arbor, 1951.

18. W. J. Pangonis, W. Heller and A. Jacobson, Tables of Light Scattering Functions for Spherical Particles; Wayne State University Press, Detroit, 1957. W. J. Pangonis and W. Heller, Angular Scattering Functions for Spherical Particles; ibid., 1960. H. Denman, W. Heller and W. J. Pangonis, Angular Scattering Functions for Spherical Particles II (α : 7.0 (0.2) $\wedge$ 5.0); ibid., 1963.

19. R. Penndorf, New Tables of Mie Scattering Functions; Geophysics Research Directorate, Air Force Cambridge Research Center, Parts 1, 2, 3, 4, 5, 6; 1958 - 1959 (m = 1.33, 1.40, 1.44, 1.486, and 1.50).

20. M. Kerker and associates, J. of Meterology, 8, 424 (1951); J. Opt. Soc. Am., 43, 49 (1953) (m = 2); ibid., 45, 1080, 1081 (1955); ibid., 51, 87 (1961); J. Phys. Chem., 65, 1713 (1961) (m = 1.60); J. Opt. Soc., Am., 52, 551 (1962).

21. Fred C. Chromey, "Evaluation of Mie Equation for Colored Spheres," (Document 6247) Washington, D. C., U. S. Library of Congress.

22. Various oral reports collected during the ICES meeting. The reader interested in a fuller account of the tabulations of Mie functions available will find a comprehensive listing up to and including 1956 on pages 167 - 171 of the book by van de Hulst (ref. 24).

22a. Möglich, F., Ann. d. Phys., 83, 609 (1927).

23. R. W. Hart and E. W. Montroll, J. Appl. Phys., 22, 376, 1278 (1951).

24. H. C. van de Hulst, The Optics of Spherical Particles; Duwser and Sons, Amsterdam 1946. Light Scattering by Small Particles; John Wiley and Sons, New York 1957.

25. W. Heller, J. Chem. Phys., 26, 920, 1258 (1957).

26. W. Heller, in 'Particle Size Analysis' in Analytical Chemistry in Nuclear Reactor Technology; U. S. Atomic Energy Commission, April, 1959 pp. 3 - 10. For quantitatively more restricted equations, see also W. Heller, J. Chem. Phys., 23, 342 (1955).

27. R. Penndorf, ibid., pp 18 - 37; see also J. Phys. Chem., 62, 1537 (1958).

28. M. Nakagaki and W. Heller, J. Chem. Phys., 32, 835 (1960).

29. Max Born and E. Wolf, Principles of Optics; Pergamon Press, London 1959. J. A. Stratton, Electromagnetic Theory, McGraw Hill Book Co., New York 1941.

30. F. T. Gucker and R. L. Rowell, Dis. Faraday Soc., 1960, pp 185 - 191.

31. W. Heller and W. J. Pangonis, J. Chem. Phys., 26, 498 (1957).

32. For fuller details, see for instance: K. A. Stacey, Light Scattering in Physical Chemistry; Academic Press, New York 1956.

33. W. Heller and H. James McCarty, J. Chem. Phys., 29, 78 (1958).

34. W. Heller and R. Tabibian, J. Coll. Sci., 12, 25 (1957).

35. W. Heller, R. Tabibian and J. N. Epel, J. Coll. Sci., 11, 195 (1956).

36. W. Heller and H. B. Klevens, Phys. Rev., 67, 61 (1945).

37. V. K. LaMer and D. Sinclair, Chem. Reviews, 44, 245 (1949); M. D. Barnes, A. S. Kenyon, E. M. Zaiser and V. K. LaMer, J. Coll. Sci., 2, 349 (1947); V. K. LaMer and M. D. Barnes, J. Coll. Sci., 1, 71 (1946); I. Johnson and V. K. LaMer, J.A.C.S., 69, 1184 (1947); M. Kerker and V. K. LaMer, J.A.C.S., 72, 3516 (1950).

38. P. Doty and R. F. Steiner, J. Chem. Phys., 18, 1616 (1950); S. H. Maron and R. Lou, J. Polymer Sci., 14, 29 (1954).

39. W. J. Pangonis, W. Heller and N. A. Economou, J. Chem. Phys., 34, 960 (1961).

40. R. M. Tabibian and W. Heller, J. Coll. Sci., 13, 1 (1958).

41. J. P. Kratohvil, G. J. Dezelic, M. Kerker and E. Matijevic, J. Polymer Sci., 57, 59 (1962).

42. M. Kerker, J. Coll. Sci., 5, 165 (1950); M. Kerker and M. Hampton, J. Opt. Soc. Am., 43, 370 (1953); M. Kerker and E. Matijevic, ibid., 50, 722 (1960).

43. W. Heller and M. Nakagaki, J. Chem. Phys., 31, 1188 (1959).

44. W. Heller and W. J. Pangonis and N. A. Economou, J. Chem. Phys., 34, 971 (1961).

45. W. Heller and R. M. Tabibian, J. Phys. Chem., 66, 2059 (1962).

46. W. Heller and M. Nakagaki, J. Chem. Phys., 30, 783 (1959).

47. M. Nakagaki and W. Heller, Preliminary Announcement in Bull. Am. Phys. Soc., 5, 28 (1960).

48. W. Heller, M. Nakagaki and M. L. Wallach, J. Chem. Phys., 30, 444 (1959).

49. W. B. Dandliker, J.A.C.S., 72, 5110 (1950).

50. Gjuro Dezelic and Josip P. Kratohvil, J. Coll. Sci., 16, 561 (1961).

51. Unpublished data by H. Doppke.

52. Results by M. L. Wallach to be published soon.

53. W. Heller, H. L. Bhatnagar and M. Nakagaki, J. Chem. Phys., 36, 1163 (1962); W. Heller and E. Vassy, Phys. Rev., 63, 65 (1943); J. Chem. Phys., 14, 565 (1946); W. Heller and H. B. Klevens, H. Oppenheimer, J. Chem. Phys., 14, 565 (1946).

54. J. B. Bateman, F. J. Weneck and D. C. Eshler, J. Coll. Sci., 14, 308 (1959).

55. B. Ray, Proc. Indian Assoc. Cult. Sci., 7, 1 (1921).

56. V. K. LaMer and I. W. Plesner, J. Polymer Sci., 24, 147 (1957).

57. A. F. Stevenson, W. Heller and M. L. Wallach, J. Chem. Phys., 34, 1789 (1961); see also M. Kekar and V. K. LaMer in Ref. 38.

58. W. L. Wallach, W. Heller and A. F. Stevenson, J. Chem. Phys., 34, 1796 (1961).

TECHNICAL REPORT DISTRIBUTION LIST

Wayne State University

Contract Nonr 3511(00) NR 051-380

	No. Copies
Commanding Officer Office of Naval Research Branch Office The John Crerar Library Building 86 East Randolph Street Chicago 1, Illinois	(1)
Commanding Officer Office of Naval Research Branch Office 346 Broadway New York 13, N ew York	(1)
Commanding Officer Office of Naval Research Branch Office 1030 East Green Street Pasadena 1, California	(1)
Commanding Officer Office of Naval Research Branch Office Box 39 Navy #100 Fleet Post Office New York, New York	(7)
Director, Naval Research Laboratory Washington 25, D.C. Attn: Technical Information Officer Chemistry Division	(6) (2)
Chief of Naval Research Department of the Navy Washington 25, D. C. Attn: Code 425	(2)
DDR&E Technical Library Room 3C-128, The Pentagon Washington 25, D, C.	(1)
Technical Director Research & Engineering Division Office of the Quartermaster General Department of the Army Washington 25, D. C.	(1)
Research Director Clothing & Organic Materials Division Quartermaster Research & Engineering Command U. S. Army Natick, Massachusetts	(1)
Air Force Office of Scientific Research (SRC-E) Washington 25, D. C.	(1)
Commanding Officer Diamond Ordnance Fuze Laboratories Washington 25, D. C. Attn: Technical Information Office Branch 012	(1)
Office, Chief of Research & Development Department of the Army Washington 25, D. C. Attn: Physical Sciences Division	(1)
Chief, Bureau of Ships Department of the Navy Washington 25, D. C. Attn: Code 342C	(2)
Chief, Bureau of Naval Weapons Department of the Navy Washington 25, D. C. Attn: Technical Library Code RRMA-3	(3) (1)
ASTIA Document Service Center Arlington Hall Station Arlington 12, Virginia	(10)
Director of Research U.S. Army Signal Research & Development Laboratory Fort Monmouth, New Jersey	(1)
Naval Radiological Defense Laboratory San Francisco 24, California Attn: Technical Library	(1)
Naval Ordnance Test Station China Lake, California Attn: Head, Chemistry Division Code 40 Code 50	(1) (1) (1)

REVISED 1 FEB 1962

B-1970

Contract Nonr 3511(00) Wayne State University NR NO. 051-380

	No. Copies
Commanding Officer Army Research Office Box CM, Duke Station Durham, North Carolina Attn: Scientific Synthesis Office	(1)
B rookhaven National Laboratory Chemistry Department Upton, New York	(1)
Atomic Energy Commission Division of Research Chemistry Programs Washington 25, D. C.	(1)
Atomic Energy Commission Division of Technical Information Extension Post Office Box 62 Oak Ridge, Tennessee	(1)
U.S. Army Chemical Research and Development Laboratories Technical Library Army Chemical Center, Maryland	(1)
Office of Technical Services Department of Commerce Washington 25, D. C.	(1)
Dr. Albert Lightbody Naval Ordnance Laboratory White Oak, Silver Spring, Md.	(1)
Dr. W. H. Avery Applied Physics Laboratory The Johns Hopkins University 8621 Georgia Avenue Silver Spring, Md.	(1)
National Bureau of Standards Washington 25, D. C. Attn: Chief, Organic and Fibrous Materials Division	(1)
Chief, Bureau of Yards and Docks Department of the Navy Washington 25, D. C. Attn: Code P300	(1)
Aeronautical Systems Division ASRCNP Wright-Patterson Air Force Base Ohio	(1)
Office of Chief of Engineers Research and Development Division Department of the Army Gravelly Point Washington 25, D. C.	(1)
Engineer Research and Development Laboratory Fort Belvoir, Virginia Attn: Materials Branch, Mr. Mitton	(1)
Commander Mare Island Naval Shipyard Rubber Laboratory Vallejo, California	(1)
Dr. J. H. Faull, Jr. 72 Fresh Pond Lane Cambridge 38, Massachusetts	(1)
Dr. R. S. Stein Department of Chemistry University of Massachusetts Amherst, Massachusetts	(1)
Dr. L. F. Rahm Plastics Laboratory Princeton University Princeton, New Jersey	(1)
Dr. A. V. Tobolsky Department of Chemistry Princeton University Princeton, New Jersey	(1)
Dr. U. P. Strauss Department of Chemistry Rutgers - The State University New Brunswick, New Jersey	(1)
Dr. Charles P. Roe Research and Development Department U. S. Rubber Company Passaic, New Jersey	(1)

Contract Nonr 3511(00) Wayne State University NR NO. 051-380

	No. Copies
ONR Resident Representative University of Michigan Ann Arbor, Michigan	(1)
National Bureau of Standards Washington 25, D. C. Attn: Dr. Victor R. Deitz	(1)
Commanding Officer Naval Air Development Center Johnsville, Pennsylvania Attn: Dr. Howard R. More	(1)
Plastics Technical Evaluation Center Pictinny Arsenal Dover, New Jersey	(1)
Dr. G. Barth-Wehrenalp, Director Inorganic Research Department Pennsalt Chemicals Corporation Box 4388 Philadelphia 18, Pennsylvania	(2)
Mr. James P. Lodge, Chief Air Pollution Chemical Research Department of Health, Educ. and Welfare 4676 Columbia Parkway Cincinnati 26, Ohio	(1)
Dr. T. G. Fox, Director of Research Mellon Institute 4400 Fifth Avenue Pittsburgh 13, Pennsylvania	(1)
NASA 1512 H Street, N. W. Washington 25, D. C.	
Dr. M. S. Cohen, Chief Propellants Synthesis Section Reaction Motors Division Denville, New Jersey	(1)
Dr. D. A. Brown Department of Chemistry University College Upper Merrion Street Dublin, Ireland	(1)
Dr. T. L. Heying Organics Division Olin Mathieson Chemical Corporation 275 Winchester Avenue New Haven, Connecticut	(1)
Monsanto Research Corporation Everett Station Boston 49, Massachusetts Attn: Mr. K. Warren Easley	(1)
Dr. B. Wunderlich Department of Chemistry Cornell University Ithaca, New York	(1)